AD-A064 310 HUGHES AIRCRAFT CO TORRANCE CALIF ELECTRON DYNAMICS DIV F/G 9/1
DIAMOND SUPPORTED HELIX FOR MILLIMETER WAVE.(U)
JAN 79 O SAUSENG, A E MANOLY, J R MENTE F30602-77-C-0188
UNCLASSIFIED EDD-W-07525-F RADC-TR-78-270 NL

1 OF 1
AD A064 310

END
DATE FILMED
4 -79
DDC

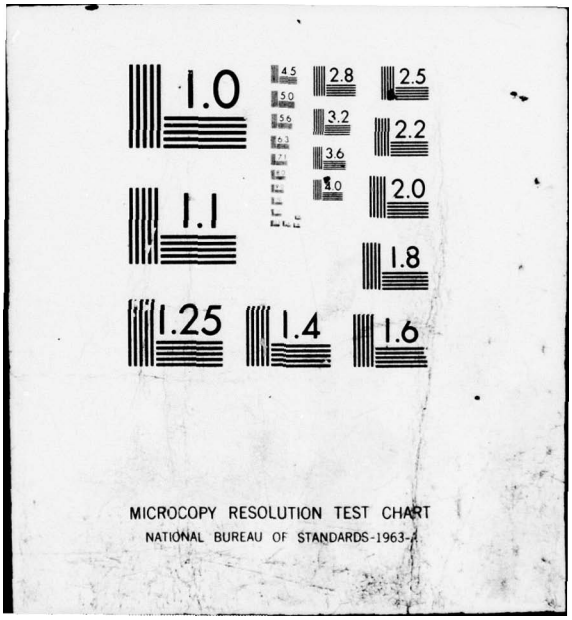
1.0
1.1
1.25
1.4
1.6
1.8
2.0
2.2
2.5
2.8
3.2
3.6
4.0
4.5
5.0
5.6
MICROCOPY RESOLUTION TEST CHART
NATIONAL BUREAU OF STANDARDS-1963-A

This report has been reviewed by the RADC Information Office (OI) and is releasable to the National Technical Information Service (NTIS). At NTIS it will be releasable to the general public, including foreign nations.

RADC-TR-79-170 has been reviewed and is approved for publication.

APPROVED: Henry Freiberg

HENRY FREIBERG
Project Engineer

APPROVED: Joseph J. Simmons

JOSEPH J. SIMMONS
Technical Director
Surveillance Division

FOR THE COMMANDER: John P. Huss

JOHN P. HUSS
Acting Chief, Plans Office

If your address has changed or if you wish to be removed from the RADC mailing list, or if the addressee is no longer employed by your organization, please notify RADC (OCTM) Griffiss AFB NY 13441. This will assist us in maintaining a current mailing list.

Do not return this copy. Retain or destroy.

UNCLASSIFIED

SECURITY CLASSIFICATION OF THIS PAGE (When Data Entered)

REPORT DOCUMENTATION PAGE

READ INSTRUCTIONS BEFORE COMPLETING FORM

1. REPORT NUMBER: RADC-TR-78-276	2. GOVT ACCESSION NO.
3. RECIPIENT'S CATALOG NUMBER	
4. TITLE (and Subtitle): DIAMOND SUPPORTED HELIX FOR MILLIMETER WAVE	5. TYPE OF REPORT & PERIOD COVERED: Final Technical Report. Aug 77 - Sep 78
6. PERFORMING ORG. REPORT NUMBER: EDD-W-07525-F	
7. AUTHOR(s): O. Sauseng, A. Hall, A. E. Manoly, J. R. Mente	8. CONTRACT OR GRANT NUMBER(s): F30602-77-C-0188
9. PERFORMING ORGANIZATION NAME AND ADDRESS: Hughes Aircraft Company, Electron Dynamics Division, 3100 West Lomita Blvd Torrance CA 90509	10. PROGRAM ELEMENT, PROJECT, TASK AREA & WORK UNIT NUMBERS: 62702F, 55730218, 17, 02
11. CONTROLLING OFFICE NAME AND ADDRESS: Rome Air Development Center (OCTP), Griffiss AFB NY 13441	12. REPORT DATE: January 1979 13. NUMBER OF PAGES: 64
14. MONITORING AGENCY NAME & ADDRESS (if different from Controlling Office): Same	15. SECURITY CLASS. (of this report): UNCLASSIFIED 15a. DECLASSIFICATION/DOWNGRADING SCHEDULE: N/A

16. DISTRIBUTION STATEMENT (of this Report)

Approved for public release; distribution unlimited.

17. DISTRIBUTION STATEMENT (of the abstract entered in Block 20, if different from Report)

Same

18. SUPPLEMENTARY NOTES

RADC Project Engineer: Henry Friedman (OCTP)

19. KEY WORDS (Continue on reverse side if necessary and identify by block number)

Thermal studies on helix structures for millimeter waves
Thermal interface conductance measurements
Thermal conductivity measurements
Thermal tests on diamond supported millimeter wave helix

20. ABSTRACT (Continue on reverse side if necessary and identify by block number)

The thermal properties of materials, that can be used for high power helix structures, were evaluated experimentally with equipment that incorporated an infrared microscope for temperature measurements.

The interface heat transfer properties between such materials were measured as a function of contact pressure and for different surface finishes. In addition the thermal conductivity of suitable ceramic materials, such as anisotropic Boron Nitride, Beryllia and Diamond was measured as a function of temperature.

DD FORM 1 JAN 73 1473

UNCLASSIFIED

SECURITY CLASSIFICATION OF THIS PAGE (When Data Entered)

Millimeter wave helix structures for 40 GHz to 50 GHz were constructed for thermal evaluation with these materials. A power handling capability of 165 watts/in. with an average helix temperature of 380°C was demonstrated with a diamond supported helix structure, indicating that helix traveling-wave tubes can be designed for RF-power levels of 100 watt to 200 watt in the 40 GHz to 50 GHz range using such a structure.

PREFACE

This final technical report was prepared by the Electron Dynamics Division, Hughes Aircraft Company, Torrance, California on Contract F30602-77-C-0188, for Rome Air Development Center, Griffiss Air Force Base, New York. It summarizes the results and efforts of this work carried out from August 1977 through September 1978. Henry Friedman (OCTP) was RADC Project Engineer.

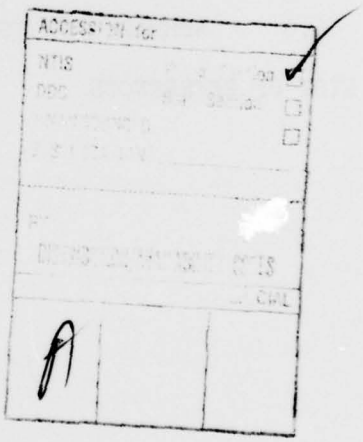

TABLE OF CONTENTS

LIST OF ILLUSTRATIONS

LIST OF ILLUSTRATIONS (CONTINUED)

LIST OF ILLUSTRATIONS (CONTINUED)

EVALUATION

This Final Technical Report covers research and development work done during the period August 1977 to September 1978 under Contract F30602-77-C-0188 on the thermal properties of materials suitable for helix structures of millimeter wave traveling wave tubes.

The objective of the program was to explore and evaluate methods of helix construction and assembly for optimum thermal design of helix assemblies for 40 to 50 GHz, 10 watt traveling wave tubes. The program also aimed to determine the thermal limits of various helix structures using experimental assemblies.

Data was obtained on thermal conductivity of ceramic materials and thermal interface resistance between ceramic and metal surfaces as functions of temperature, pressure, and surface finish. Ceramic materials investigated were beryllia, anisotropic boron nitride and diamond.

The work accomplished under this contract supports the Air Force C^3 mission by providing data not previously available, that can be used for the thermal design and analysis of high power helix structures for traveling wave tubes used in radar, communications and ECM equipments.

Henry Friedman

HENRY FRIEDMAN (OCTP)
Project Engineer

1.0 INTRODUCTION

The RF power capability of traveling wave tubes at CW becomes rapidly smaller when they are designed to operate at very high frequencies, especially in the millimeter range. Frequency scaling of the TWT designs requires that the dimensions of electron beam and slow wave structure be significantly smaller with higher frequencies. This makes it necessary to decrease the beam power and RF power levels so that the power densities of the associated heat losses remain within acceptable limits. For this reason the available beam power has to be reduced of higher frequencies approximately in proportion to the square of frequency. The electronic (beam conversion) efficiency becomes then lower also, and is further degraded by the higher RF-losses at higher frequencies. A more rapid drop in RF-output power has therefore to be expected at higher frequencies.[1]

The power capability of helix tubes is limited primarily by three factors:

One is that helix tubes tend to become unstable (backward wave oscillations) at excessively high beam power levels and beam voltages, especially when they are designed for large bandwidth. For this reason there is a practical upper limit for the design voltage (and power) of a helix tube in the order of

$$V_{max} \approx 10 \text{ Kv to } 12 \text{ Kv}$$

The other well known limitation for traveling wave tubes in general is that the operating temperatures inside the tube must not exceed certain limits if good tube performance is to be achieved with reasonable life and reliability. Even though helices can be fabricated of refractory metals with very high melting temperatures (tungsten 3400°C, molybdenum

2600°C) it was found that a maximum operating temperature of the helix of about

$$T_{maximum}\ (helix) \approx 400^{\circ}C$$

should not be exceeded. Heat transfer by radiation is then negligible and has to depend primarily on conduction. Conduction cooled helix tubes may then operate with temperature gradients ΔT from the heat sink to the helix of up to

$$\Delta T_{max} \approx 300^{\circ}C$$

(see Section 4). The third power limitation of helix tubes is imposed by the need to insulate the helix electrically with ceramic support rods. The ceramic support structure restricts the heat transfer from the helix to the outside of the tube (heat sink), and thus limits the power capability of the tube.

Major technological advancements in heat transfer capability of the helix support structure have been made over a number of years, and substantially higher power levels can therefore be achieved with such tubes. Early helix tubes with glass envelopes[2,3] were converted to all-metal structures where the helix was supported by alumina rods inside a flexbile metal envelope that compressed the helix structure (triangulation method). Further improvements were obtained when alumina was replaced by Beryllia ceramics with better thermal conductivity.[4] It was found however that the interface between helix and ceramic rods, and between ceramic rods and tube envelope presented serious obstacles to improve the heat flow further. For this reason all-brazed helix structures were developed, where the rod to helix and the rod to envelope interfaces were brazed.[5] This method was expected to eliminate thermal interface resistances. Brazing the rods to the helix as well as to the tube

envelope was found to be difficult and involves complex technology. The tube envelope has to match the thermal expansion of the Beryllia rods in order to avoid destructive stress in the rods. This can be accomplished by constructing the tube envelope with specially selected metals with a composite thermal expansion that matches that of Beryllia ceramics. Brazing of Beryllia ceramics to metals requires elaborate procedures for metallizing. The brazing causes large increases in RF-circuit losses because most brazing alloys have very high resistivity. It was found to be difficult to control the reliability of the rod brazes. One weak brazing joint will produce a hot spot that can readily destroy the helix. These problems are compounded at higher frequencies. Therefore more reliable thermal helix assembly techniques have been developed and the all-brazed construction technique has been replaced at Hughes EDD by the heat-shrink assembly technique. This method produces a helix assembly with high compression forces, that are much larger than those of the triangulation method, and therefore the thermal interface resistances are substantially reduced. In addition Boron Nitride ceramic material has been introduced with improved qualities. This material, unlike Alumina or Beryllia, is relatively soft and deforms slightly at the interface surfaces during assembly as a result of the high compression forces. Therefore it produces excellent thermal contacts at these surfaces. There are several types of Boron Nitride ceramics. The one most often used in helix tubes has anisotropic properties, so that high thermal conduction is obtained in one plane. The thermal conductivity in this case is practically independent of temperature, while conventional ceramics such as Alumina and Beryllia rapidly deteriorate in their thermal capability with higher temperatures. At operating temperatures the thermal conduction of anisotropic Boron Nitride is then approximately the same as that of Beryllia. In high power helix tubes it was therefore found, that a heat-shrink assembled helix structure supported by anisotropic Boron Nitride rods can be thermally comparable with an all-brazed helix structure with Beryllia rods, and will exhibit

significantly lower RF losses. The compression strength of anisotropic Boron Nitride is however much lower than that of conventional ceramic materials such as Alumina or Beryllia. It is possible in a heat shrink assembly to exceed the compression strength of Boron Nitride, and as a result, these rods will delaminate, unless the magnitude of the interference fit and its tolerances are very precisely controlled.

The heat shrink assembly technique requires therefore very high precision, but it proves to be very reliable in production.

Heat shrink assembly techniques made it also possible to improve the focusing configuration by integrating the focusing pole pieces directly into the tube envelope. This results in very accurate pole piece alignment and improved focusing, because the pole pieces are also closer to the electron beam.

2.0 OBJECTIVES OF PROGRAM

The objectives of this program are twofold. One is to explore and to evaluate methods of helix circuit construction and assembly that show promise of significantly advancing further the thermal capability of such structures. The other is to arrive at an optimum thermal design for a specific helix configuration intended for 10 W operation in the 40 GHz to 50 GHz range and to demonstrate the thermal limits of such a structure with experimental helix assemblies.

For this purpose special thermal test equipment has been developed that is capable of measuring the thermal conductivity of ceramic materials as a function of temperature. Of particular interest are comparison data of ceramic materials that have been used for high power helix assemblies such as high purity Beryllia and anisotropic Boron Nitride and of new materials that have promise of substantially better heat transfer capability and that can be considered for millimeter helix tubes, such as diamonds (IIA) or plasma-sprayed Beryllia in conjunction with composite metal ceramic helix structures[6].

In addition this test equipment has been designated to evaluate thermal resistances between ceramic and metal surfaces as a function of contact pressure. Such data are of importance for the design of helix assembly structures, where the interfaces between helix and ceramic support structures and between support structures and inner wall of the tube envelope are important factors for their heat transfer capability, particularly when the heat shrink assembly technique is used. The heat shrink assembly techniques permits to select a specified interference fit, and the magnitude of the contact pressure between the metal ceramic interfaces can therefore be controlled by the choice of the interference fit.

However no useful data have so far been available on the effects of pressure on the respective thermal resistances of such interfaces, and the selection of a suitable interference fit for heat shrink assembly was more or less a best guess. With such data it is now possible to design helix circuits for optimum heat transfer capability.

It has been known that the thermal resistance of an interface between materials depends not only on the contact pressure, but also on the flatness and surface smoothness (asperity) of the corresponding surfaces[3,4]. In general the heat transfer is found to substantially improve when the surface finish (micro-finish) is of higher quality.

A series of thermal interface resistance measurements are therefore to be carried out as a function of pressure, where the effects of surface finishes are to be evaluated. For this purpose surface finishes presently used for helix assemblies are to be compared with higher quality finishes (polished surfaces) that are expected to improve thermal resistance of such interfaces further. These data are also expected to provide guidance for an optimum thermal design of a helix structure with heat shrink assembly.

Based on this information several helix testers are to be built that are designed and constructed to represent an actual structure for operation in the 40 GHz to 50 GHz range. The design is to be optimized with respect to heat transfer capability, with one tester each using Boron Nitride, Beryllia and diamond support materials. The testers are to be provided with either DC-couplers or RF-couplers so that either DC-heating or RF-heating using a high power driver tube can be applied. For each of these testers the maximum dissipation power is to be determined by increasing the power load to their destructive level, so that the best design and its power capability can be experimentally established and verified.

3.0 MEASUREMENT OF THERMAL INTERFACE CONDUCTANCE AND THERMAL CONDUCTIVITY

3.1 DESIGN AND FEATURES OF THERMAL TESTER

Thermal test equipment has previously been used at Hughes EDD for the design of high power helix structures. The design of the equipment and its measurement techniques was established following the approach described by NASA Lewis Research Center.[7] The equipment is provided with a vacuum envelope to eliminate errors due to convection cooling, and to prevent oxidation of surfaces. Test samples are inserted between two axially aligned columns that are provided with heaters. One of the columns is axially movable and can be pressure loaded by an external shaft that is sealed by O-rings. The other column is attached to a watercooled heat sink. The pressure is monitored by a gauge, and temperature distributions can be measured with thermocouples.

The design of the equipment has been modified to improve its accuracy and to extend its temperature range to about 500°C max and its pressure range to 40,000 psi max. More accurate bearings for the movable column are used, and temperature distributions are primarily monitored through a viewing window by an Infrared Microscope (Barnes Engineering Model RM-2B), that can measure surface temperatures with an accuracy of ±0.5%C. The microscope has interchangeable optics. The optics being used provides a spot size resolution of 0.0028 in. diameter. The microscope is equipped with a platform that can be moved in two lateral axis by precision micrometer drives. The tester is attached to the platform, so that accurate temperature measurements on the test samples can be made along the axis. The surfaces of the test samples are coated with carbon, and the emissitivity of the surface is calibrated with thermocouples.

A schematic of the thermal tester is shown in Figure 1.

G4381

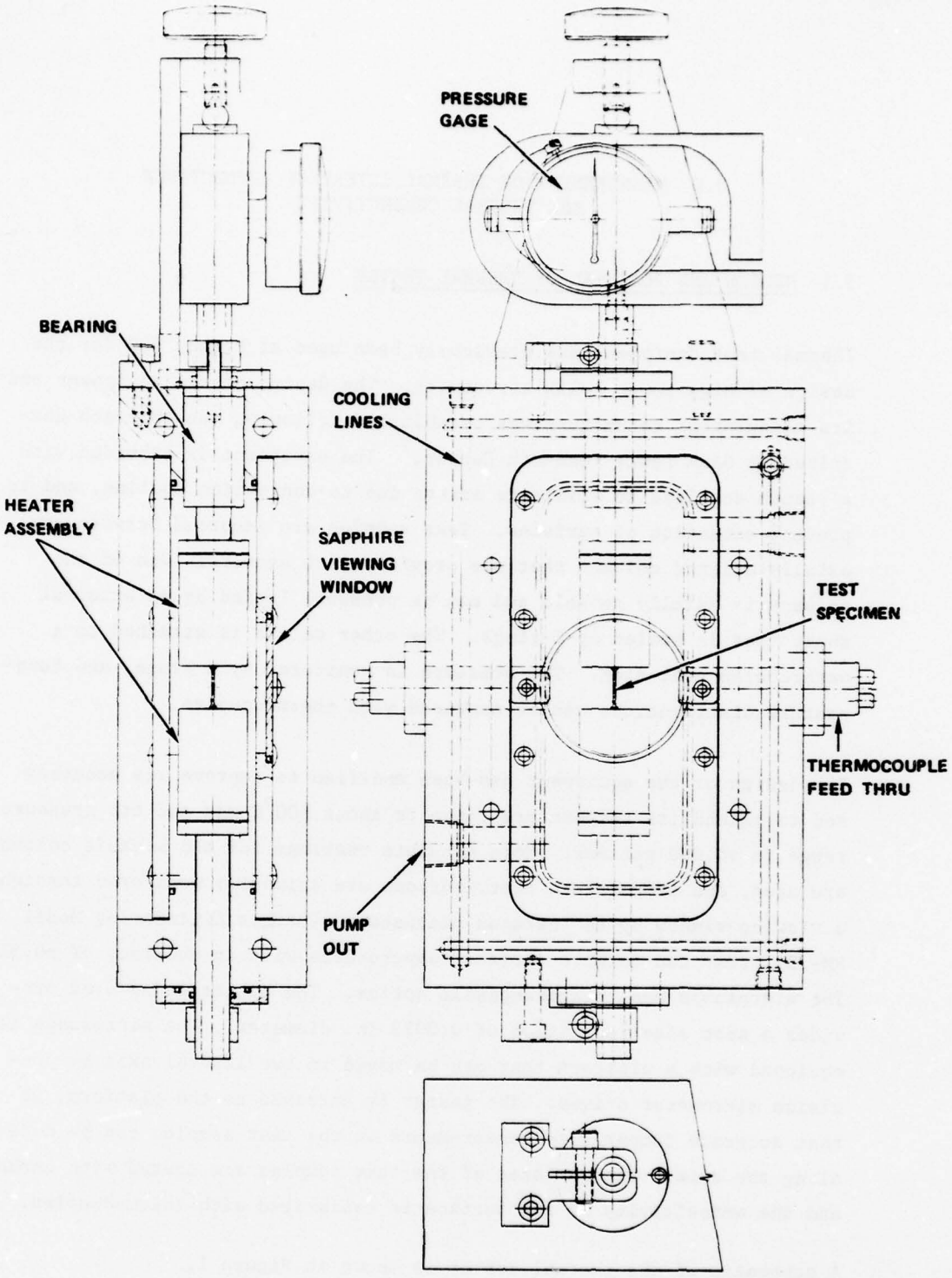

Figure 1 Schematic of thermal tester.

The test sample cross section has been selected to be 1 mm^2 (square). For accurate results it is important that the test surfaces have a high degree of flatness, that can easier be achieved on small samples. The pressure is applied by a threaded spindle through a precision ball-bearing bushing with an O-ring vacuum seal on the shaft. The pressure gauge can be interchanged by a larger one when higher pressure ranges need to be monitored.

Heat can be applied independently from the two opposite sides of the test sample so that the amount of the heat flow (temperature gradients) can be selected independent of the selected test temperature. A schematic of the heater assembly is shown in Figure 2. The heater and the tungsten probe temperatures are monitored with thermocouples. The heater assemblies are double heat-shielded both on the front and side surfaces to minimize errors in heat flow measurements due to radiation effects from the heater. The heater assemblies incorporate a heat choke to minimize axial heat losses to improve the heater efficiency. Figure 3 shows a top view of the thermal tester. The heaters with heat-shields and test probes with an attached thermocouple can be seen. Figure 4 shows a picture of the thermal tester attached to the infrared microscope and associated instrumentation.

3.2 HEAT TRANSFER DATA ON METAL-CERAMIC INTERFACES

The amount of heat flux that can be conducted through the interface of two materials is known to be a function of[7-15]

1. Contact pressure

2. Macroscopic flatness and parallelism of surfaces

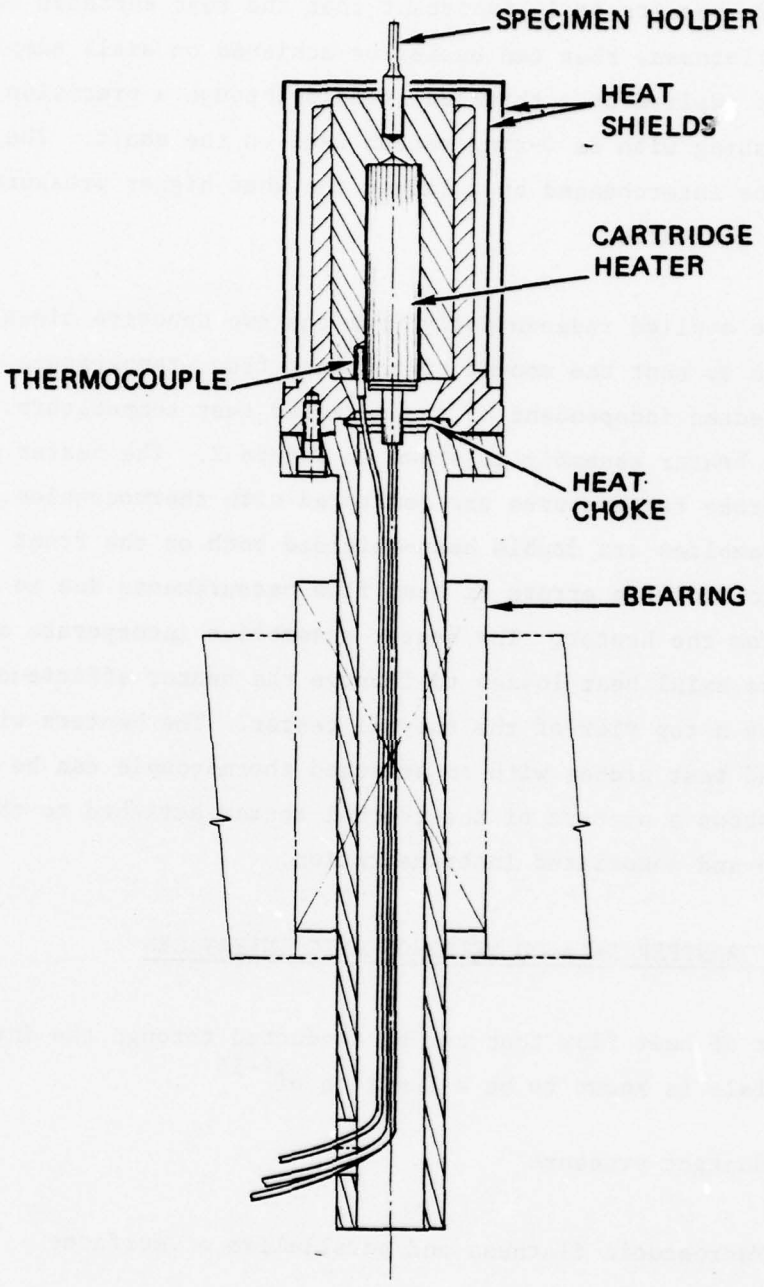

Figure 2 Schematic heater assembly for thermal tester.

E1852

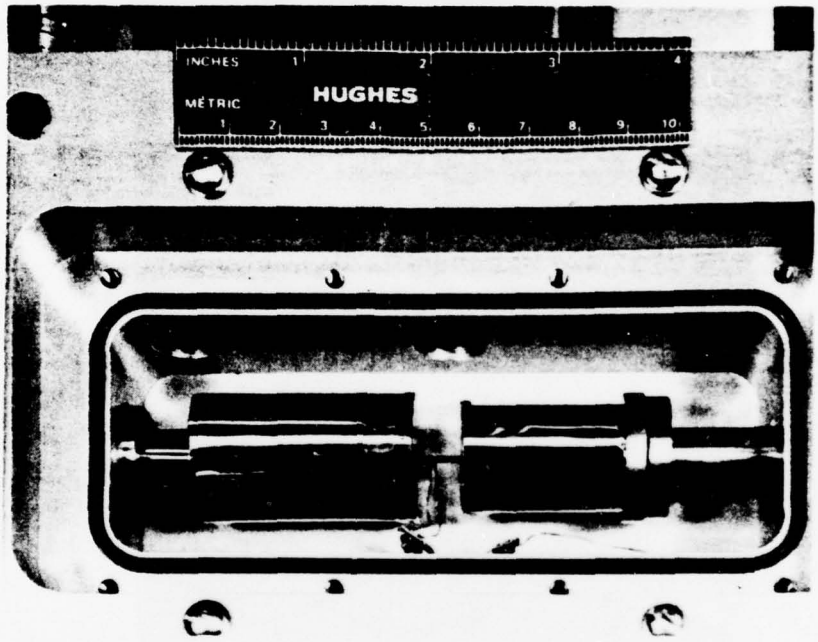

Figure 3 Top view of thermal tester (heaters with heat shields and test probes with thermocouples).

E1853

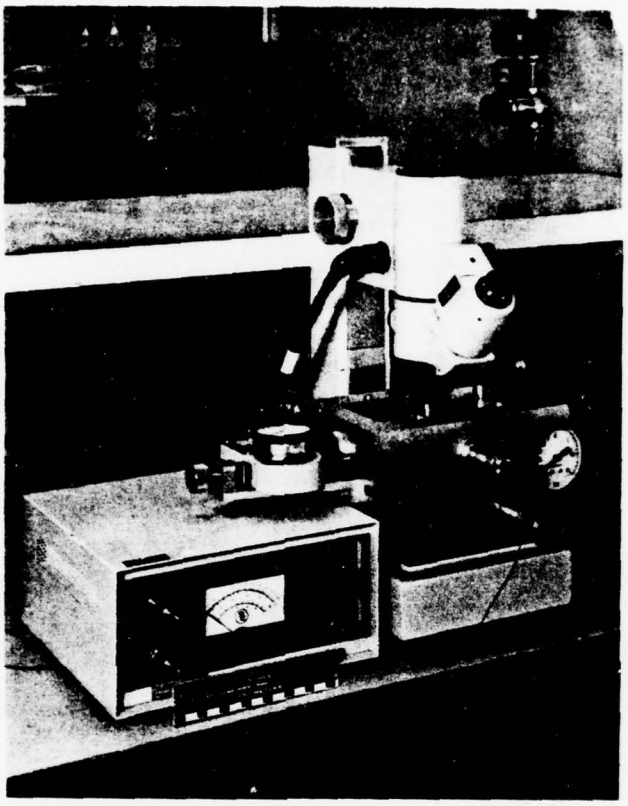

Figure 4 Picture of thermal test apparatus with infared microscope and instrumentation (radiation meter, pressure gauge and flow meter).

3. Microscopic smoothness (asperity) of surfaces

4. Mechanical properties (compliance, yield strength)

The objective of these experiments was primarily to evaluate the heat transfer capability of materials to be used for high power helix circuit construction as a function of their contact pressure and of their surface smoothness so that helix structures can be designed with better thermal capability.

It was therefore attempted to eliminate effects of imperfect parallelism and flatness in the experiments. This was however difficult to achieve even with the very carefully controlled experimental conditions, and these problems will be of concern in the construction of actual helix structures.

Heat transfer experiments were selected to evaluate the effects of surface smoothness (microfinish) such that both conventional surface finishes (usually ground) and improved (polished) surfaces were used on the samples. Ceramic materials of interest were diamond, anisotropic Boron Nitride, hot pressed Beryllia and plasma-sprayed Beryllia. Anisotropic Boron Nitride was always used in the "a" direction (higher thermal conductance). Figure 5 shows a picture of several such test samples. Selected metals were copper and copper plated tungsten. Tungsten is a preferred material for helices compared to molybdenum because of its better thermal conductivity and stronger mechanical properties, although the thermal interface properties of tungsten and molybdenum are expected to be nearly the same with the same surface conditions.

The tungsten samples have been copper-coated to simulate the actual helix interface conditions. Helices are commonly copper-coated to reduce the circuit losses and possibly to improve thermal interface conditions.

E1834

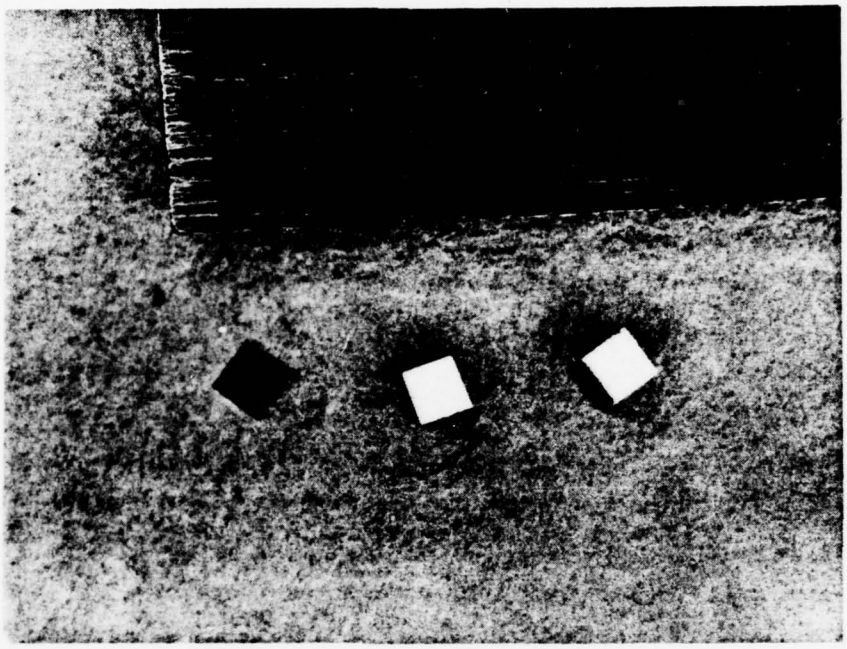

Figure 5 Ceramic test samples for thermal conductivity measurements. (Diamond, hot pressed Beryllia, plasma sprayed Beryllia on copper strip.)

The copper coating is applied to the helices with a thermal vacuum evaporation process (vacuum deposition) that achieves a chemically pure copper coating with excellent adherence. The coating thickness is in the order of 0.0002 to 0.004 inches. The surface finish is then found to be primarily determined by the structure of the base material (tungsten). Length of the test samples was 1 mm and 2 mm.

Figure 6 shows a typical measured temperature profile along the test sample. The temperature profiles are seen to be linear with distance, indicating that errors due to radiation losses are negligible. Deviations from linearity near the interfaces are very small and indicate the alignment between the samples is excellent.

The temperature slope

$$\frac{dT_p}{dZ}$$

of the probe (W) serves to determine the heat flow Q from its known thermal conductivity k_p

$$Q = k_p A \frac{dT_p}{dZ}$$

with A = cross section of material. The conductivity k_c of other materials is then obtained from their temperature slope dT_c/dZ

$$k_c = \frac{Q}{A} \frac{dT_c}{dZ}$$

The interface conductivity k_{cm} between samples is derived from their temperature drop ΔT_{cm} as

$$k_{cm} = \frac{Q}{A} \Delta T$$

It was found that the interface conductivity was practically independent of temperature. These data were taken at temperatures in the range of about 150° to 250°C. The interface conductivity is generally found to increase strongly with contact pressure. In several experiments hysteresis effects as a function of pressure were explored; data were taken both while the pressure was increased, and then when it was decreased. Although there were small differences in results, these were generally smaller than the estimated measurement accuracy.

In the initial experiments data were found to vary considerably when the experiments were repeated with reassembled samples. This was attributed to small tolerance effects in probes and test samples that would cause deviations in parallelism of surfaces. It was attempted to eliminate or reduce these effects with the insertion of copper shims between probes and test samples, as indicated in Figure 6. Data obtained with such copper shims generally gave larger heat transfer results, indicating improvements in parallelism. In some experiments such improvements were found to be quite large, as shown in Figure 7 for polished diamond to polished tungsten where the heat transfer was almost an order of magnitude larger with copper shims.

Improved heat transfer is expected with smoother surfaces of materials. This was generally confirmed as shown with the diamond/tungsten data (Figure 8); Beryllia/tungsten data (Figure 9) and Boron Nitride (Figure 10).

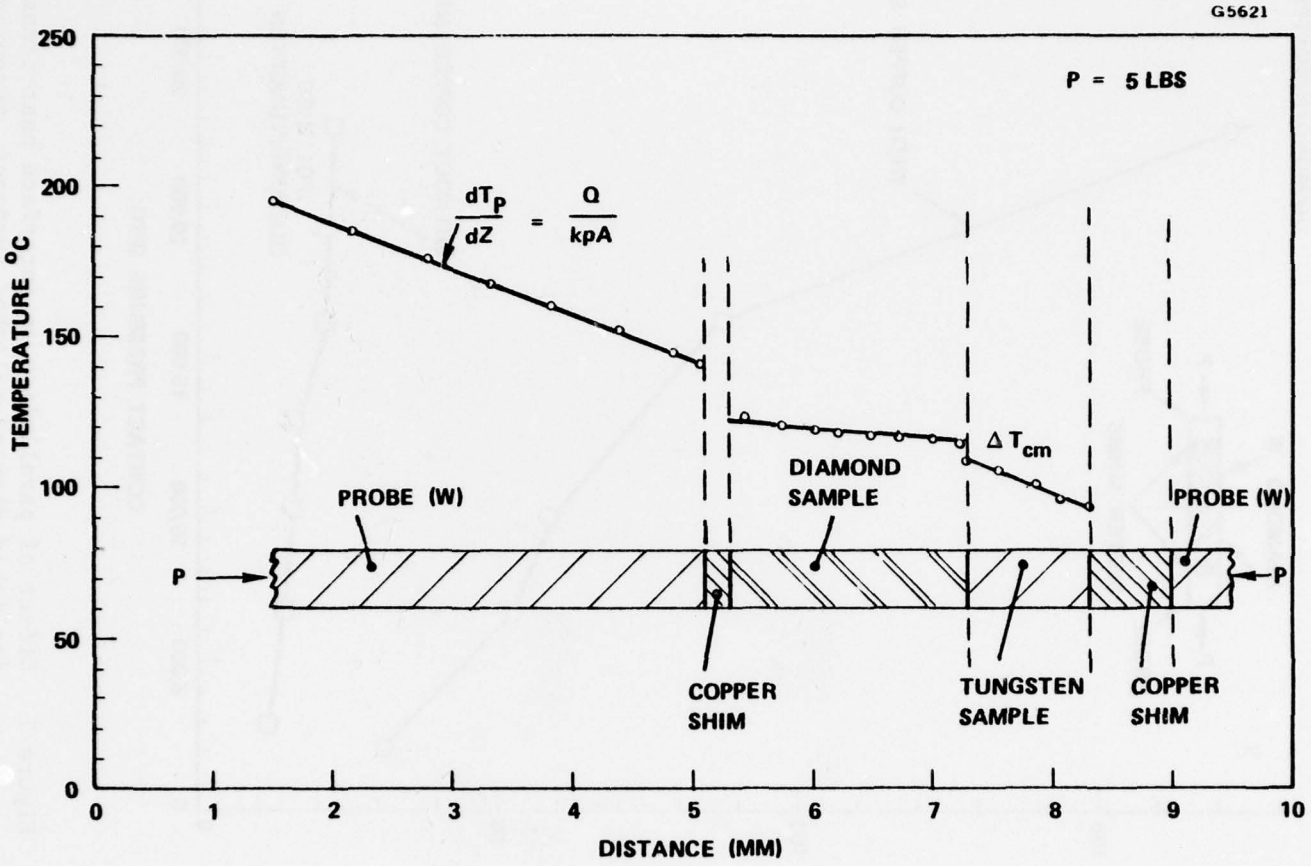

Figure 6 Temperature profiles on test samples (measured).

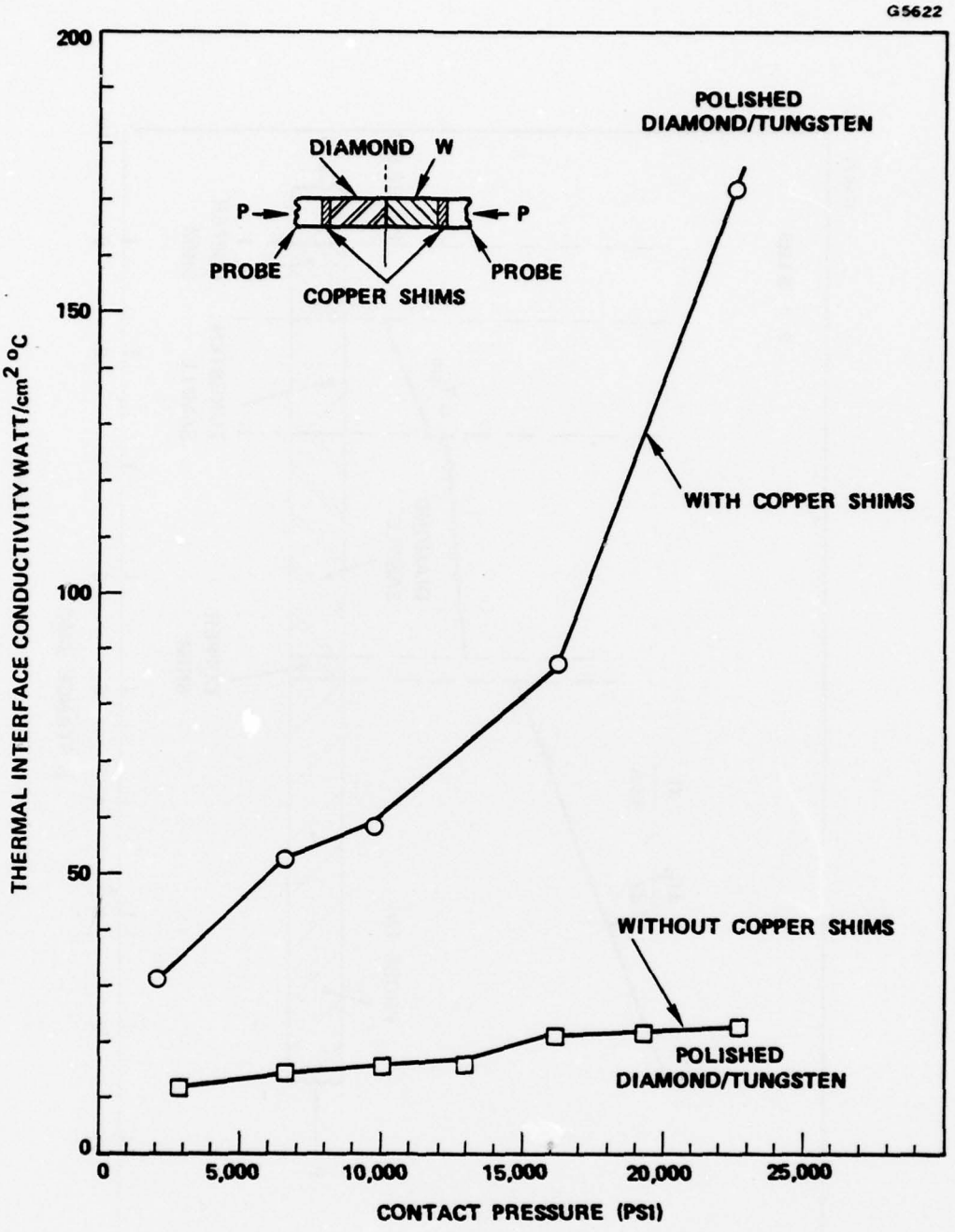

Figure 7 Effect of parallelism on interface heat transfer (polished diamond-polished tungsten, measured).

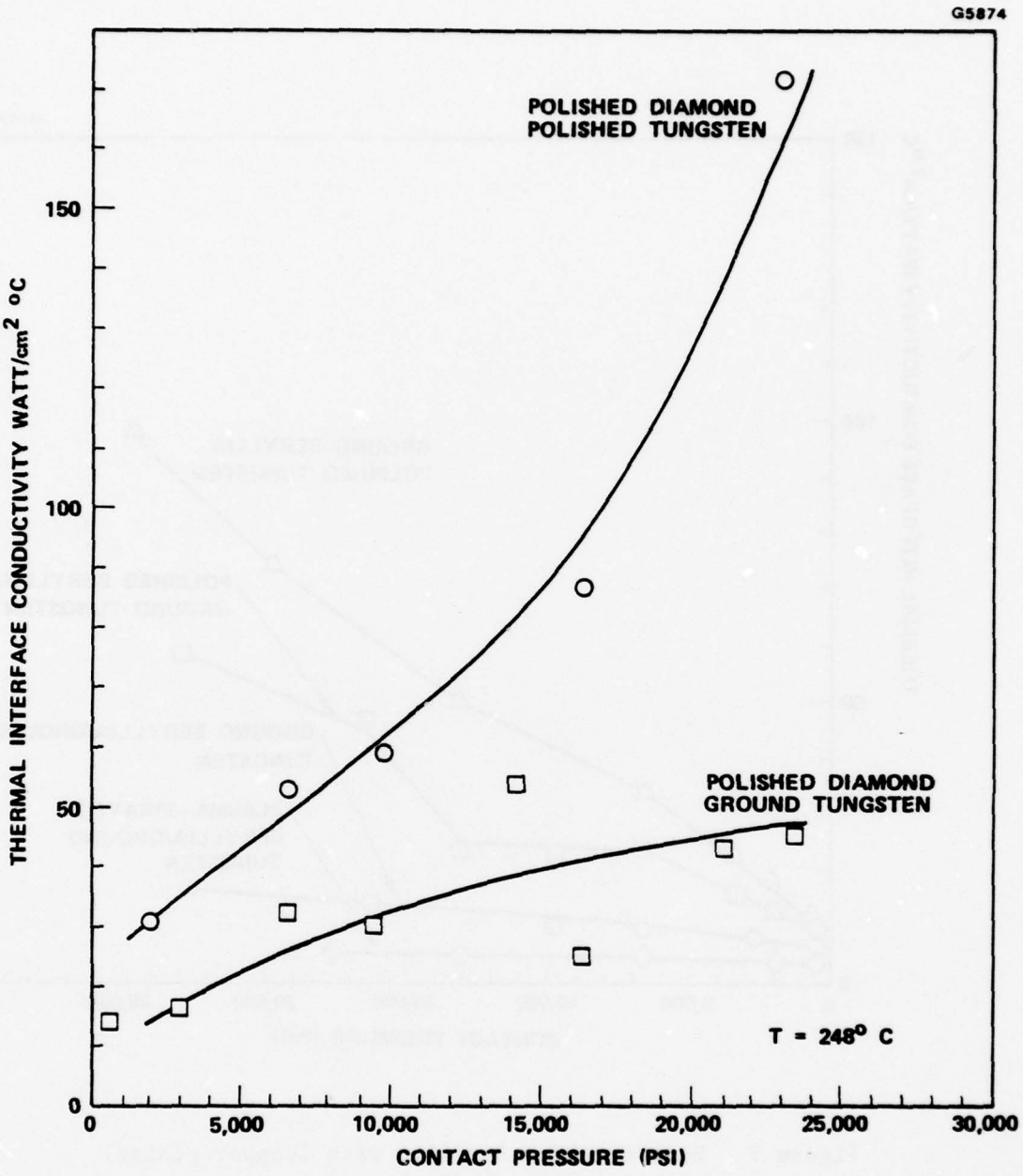

Figure 8 Heat transfer polished diamond with (copper plated) tungsten (measured).

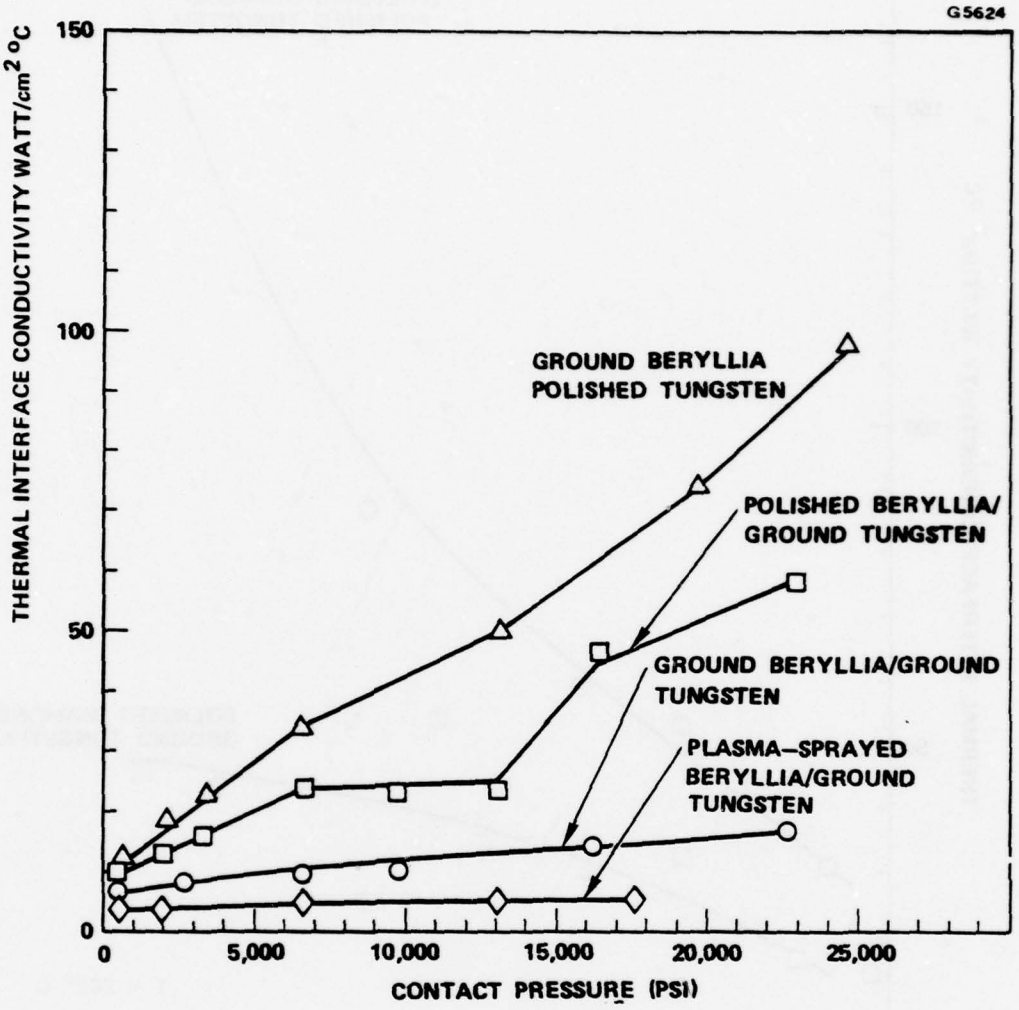

Figure 9 Heat transfer Beryllia with (copper plated) tungsten (measured).

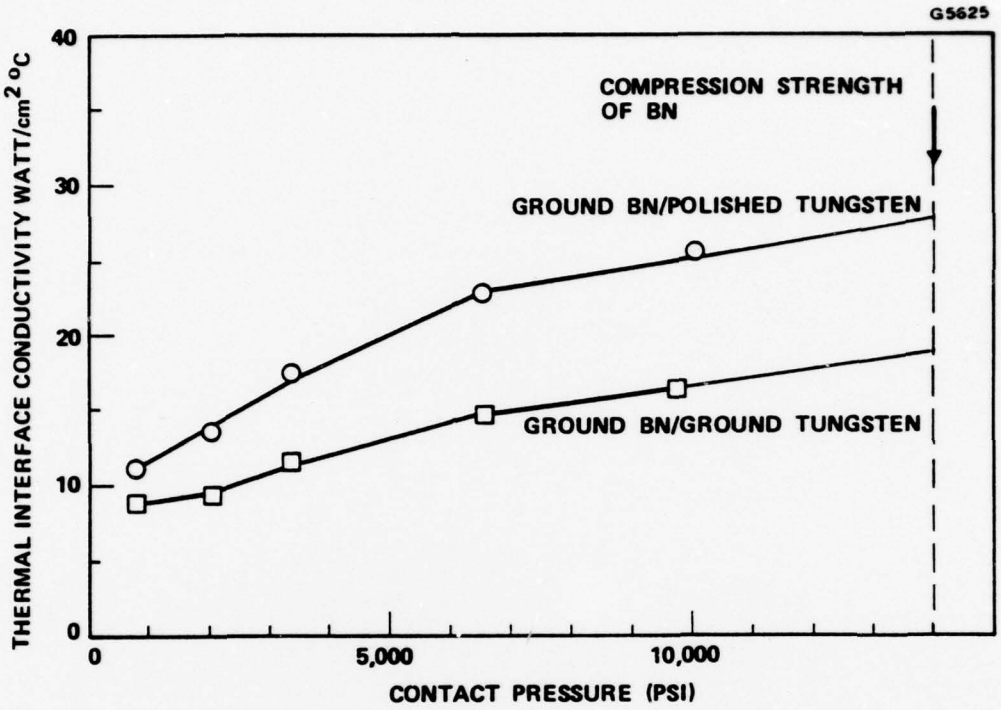

Figure 10 Heat transfer anisotropic Boron Nitride with (copper plated), tungsten (measured).

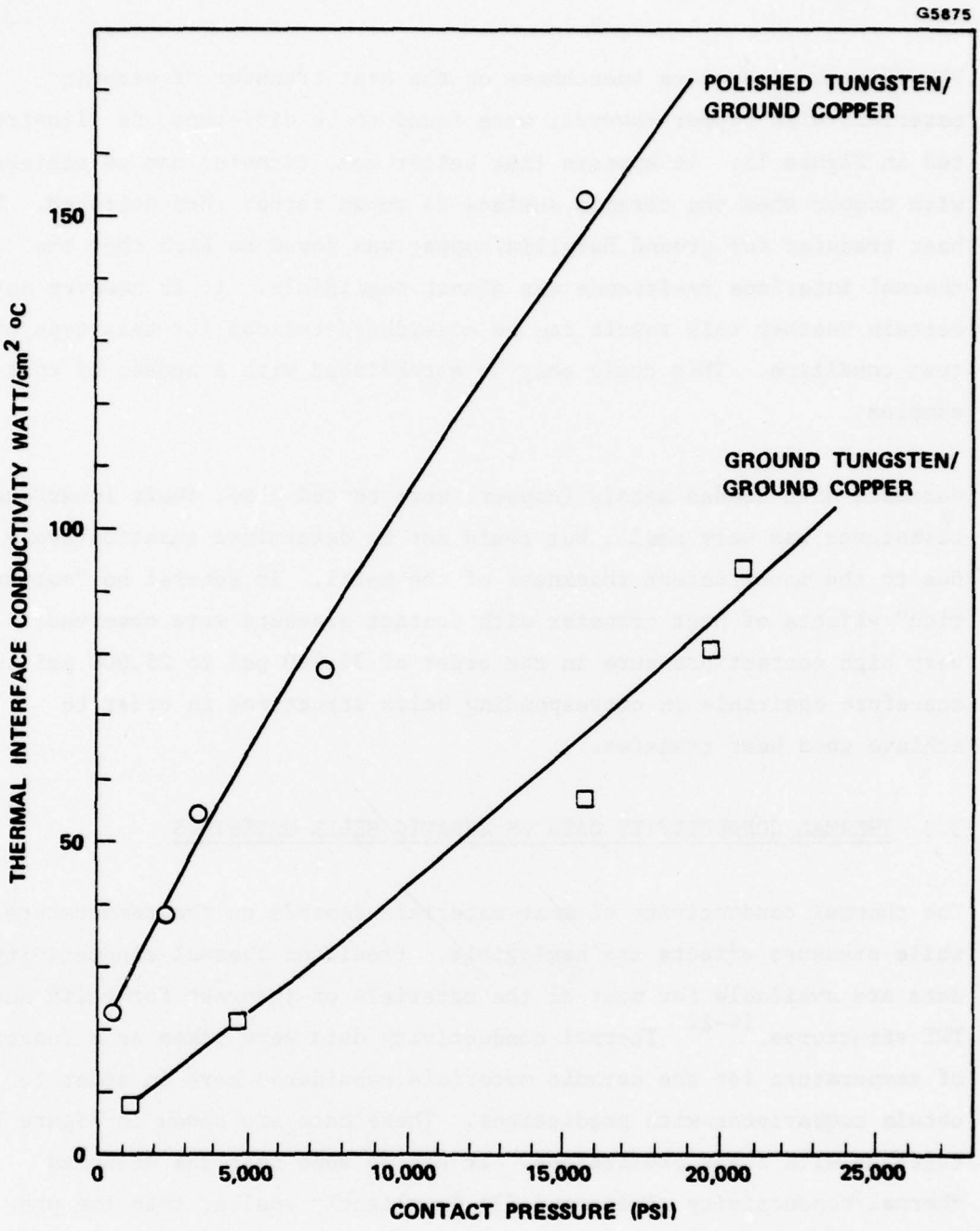

Figure 10a Heat transfer between tungsten and copper (measured).

The effects of surface smoothness on the heat transfer of ceramic materials with copper however, were found to be different, as illustrated in Figure 11. It appears that better heat transfer can be achieved with copper when the ceramic surface is rough rather than polished. The heat transfer for ground Beryllia/copper was found so high that the thermal interface resistance was almost negligible. It is however not certain whether this result can be considered typical for this type of test condition. This could only be established with a number of test samples.

Ceramics with bonded metals (copper) were tested also; their interface resistance was very small, but could not be determined quantitatively due to the insufficient thickness of the metal. In general no "saturation" effects of heat transfer with contact pressure were observed; very high contact pressure in the order of 20,000 psi to 25,000 psi is therefore desirable in corresponding helix structures in order to achieve good heat transfer.

3.3 THERMAL CONDUCTIVITY DATA ON CERAMIC HELIX MATERIALS

The thermal conductivity of most materials depends on the temperature, while pressure effects are negligible. Predicted thermal conductivity data are available for most of the materials of interest for helix and TWT structures.[16-21] Thermal conductivity data were taken as a function of temperature for the ceramic materials considered here in order to obtain comparisons with predictions. These data are shown in Figure 12 together with their predictions. It can be seen that the measured thermal conductivity of diamond IIA is slightly smaller than the predicted one (by supplier), and that for hot pressed Beryllia is within the range of its predictions. The data show that the thermal conductivity of plasma-sprayed Beryllia is approximately half of that of hot pressed Beryllia. This could be explained by a lower density of the

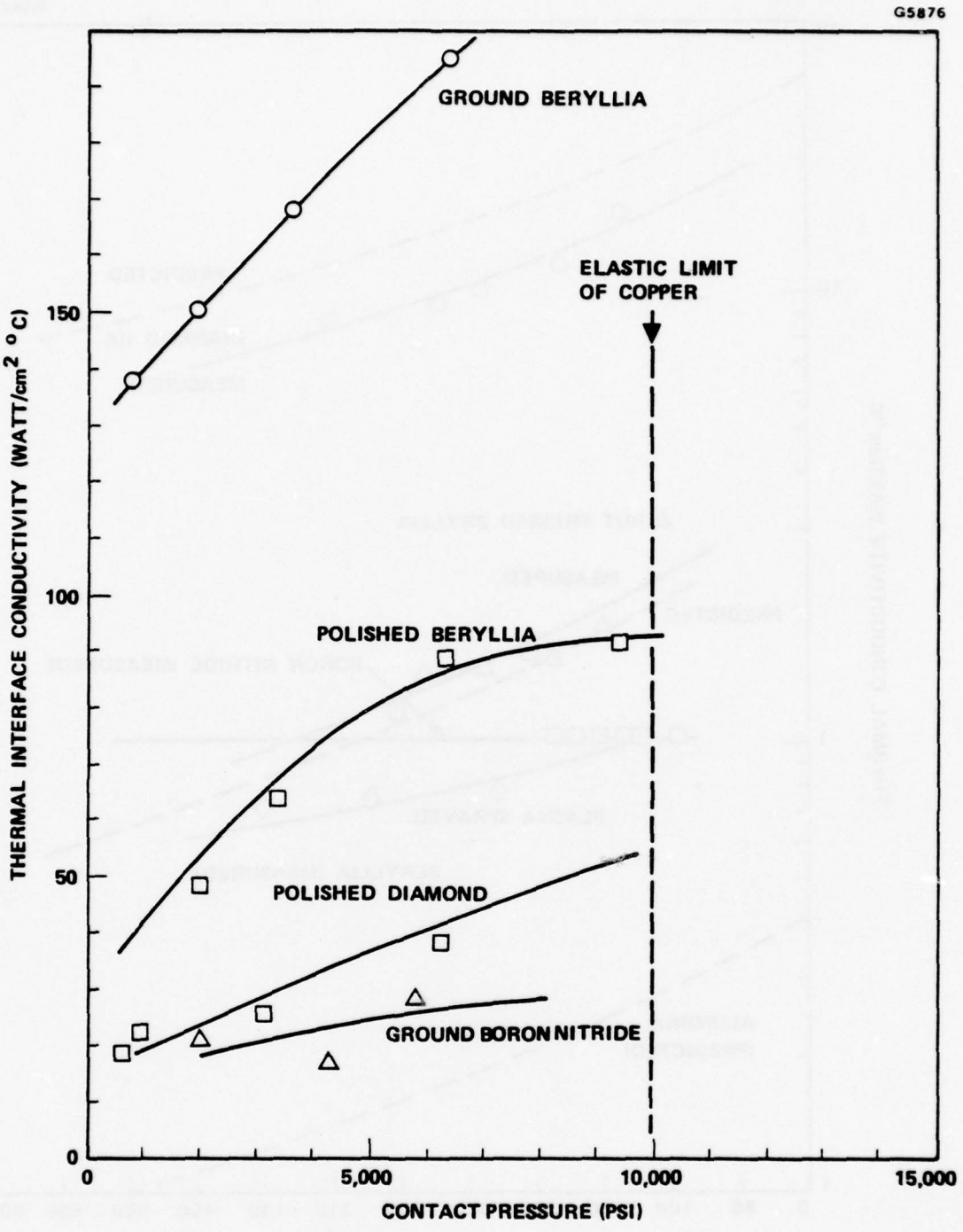

Figure 11 Heat transfer ceramic materials with ground copper (measured).

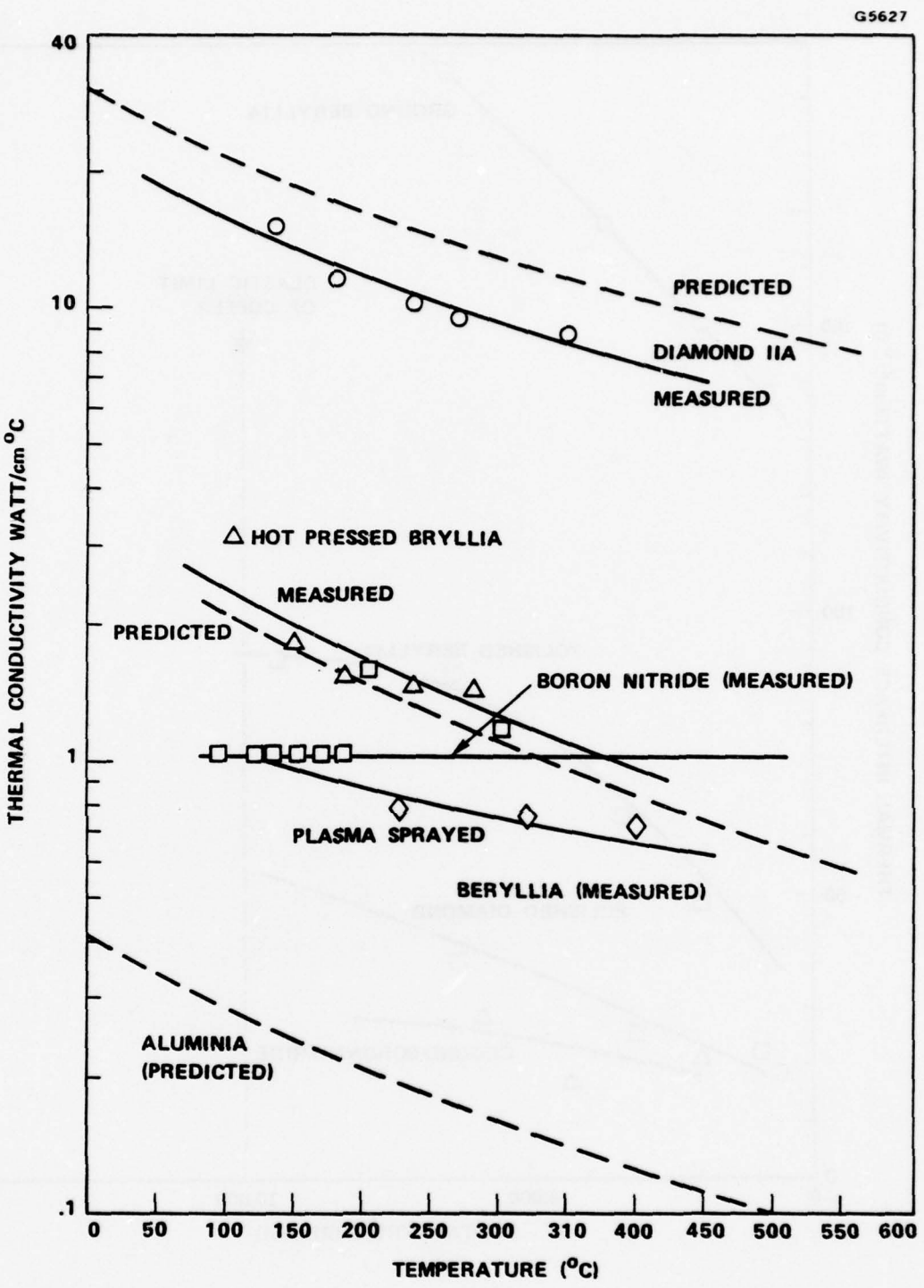

Figure 12 Thermal conductivity of ceramic materials as function of temperature (measured).

material, that would reduce the thermal conductivity as predicted in Figure 13. It can be seen that a relative density of 85% of the theoretical value would reduce the thermal conductivity by a factor of two. This is still substantially better (by a factor of about 5) than the predicted thermal conductivity of Alumina.

The density values for the Beryllia samples were measured to:

Hot-pressed Beryllia	2.80 g/ccm
Plasma sprayed Beryllia	2.64 g/ccm
Theoretical density Beryllia	3.01 g/ccm

It is not certain whether the measured data for plasma sprayed Beryllia are typical for this material. It was attempted to evaluate thermally other new ceramic materials, that appear promising for this purpose. Such materials under development are cubic Boron Nitride, that is expected to be significantly better thermally than the presently available pyrolytic Boron Nitride, and "sintered diamond" material. These materials were not available at the time of this program.

For reference purposes the thermal conductivities of some of the metals used in TWT construction are shown in Figure 14 also.

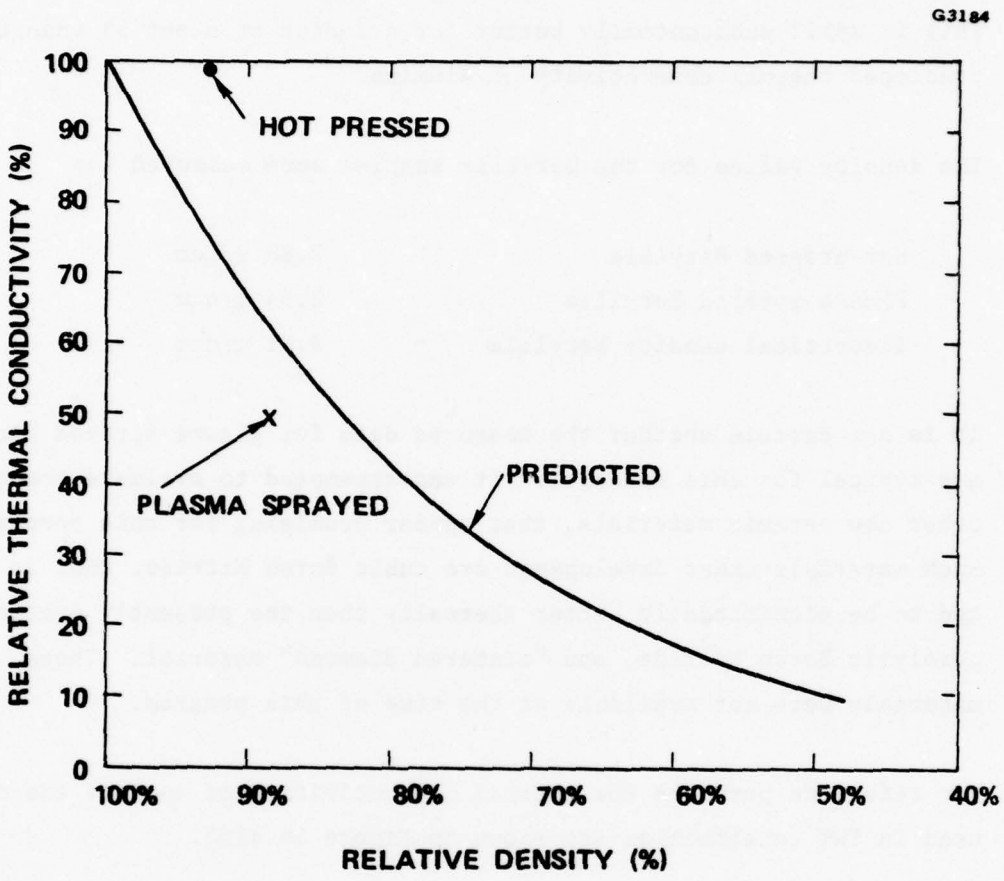

Figure 13 Thermal conductivity of Beryllia ceramics as function of density.

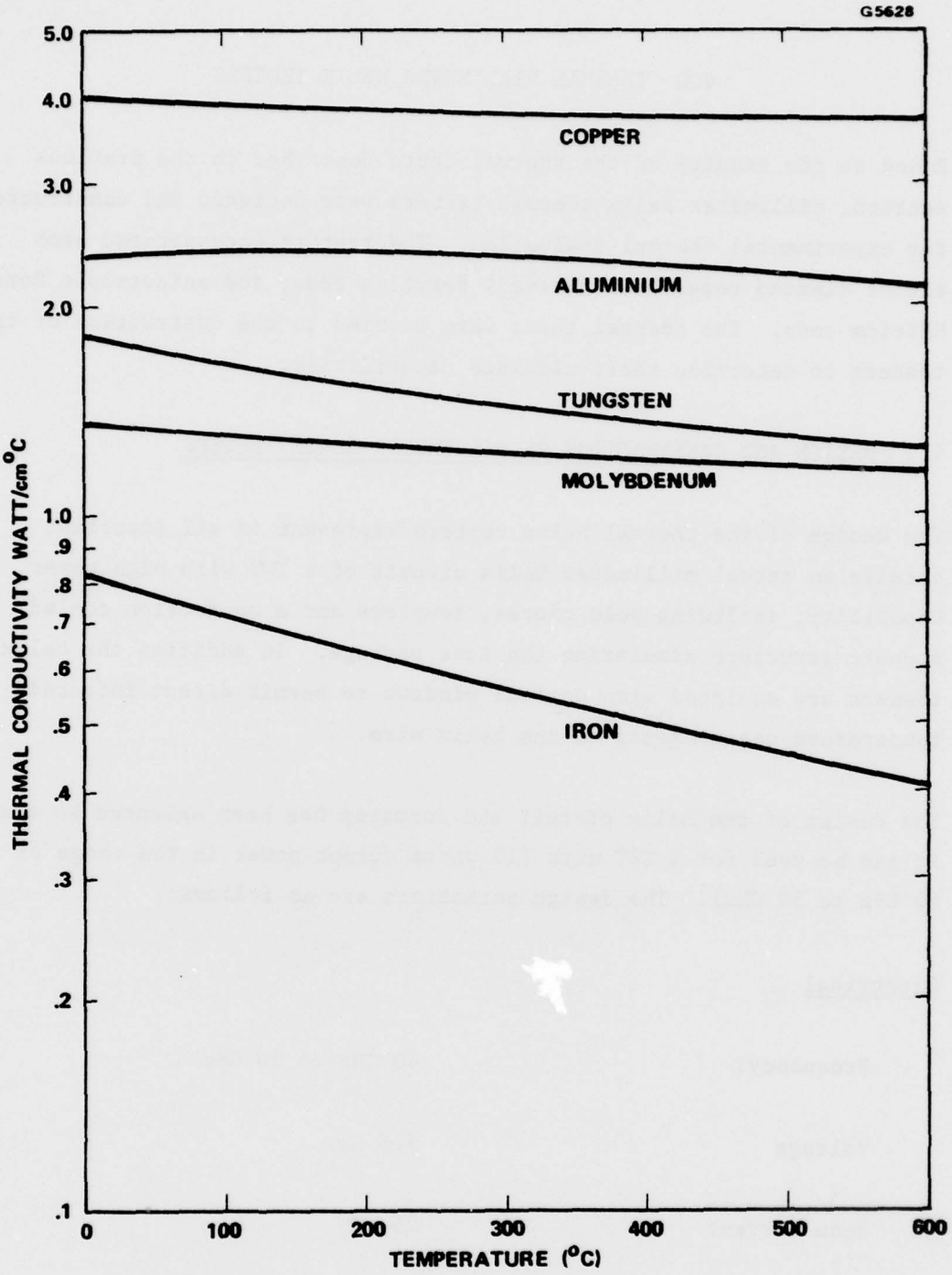

Figure 14 Thermal conductivity of metals as a function of temperature.

4.0 THERMAL MILLIMETER HELIX TESTERS

Based on the results of the thermal tests described in the previous section, millimeter helix thermal testers were designed and constructed for experimental thermal evaluation. The testers incorporated each either diamond rods, (hot pressed) Beryllia rods, and anisotropic Boron Nitride rods. The thermal tests were carried to the destruction of the testers to determine their ultimate capabilities.

4.1 DESIGN AND CONSTRUCTION OF MILLIMETER HELIX TESTERS

The design of the thermal helix testers represent in all important details an actual millimeter helix circuit of a TWT with high power capability, including pole pieces, couplers and a conduction cooled support structure simulating the tube package. In addition the helix testers are equipped with optical windows to permit direct infrared temperature measurements on the helix wire.

The design of the helix circuit and focusing has been selected so that it can be used for a TWT with (10 watts output power in the range of 40 GHz to 50 GHz). The design parameters are as follows:

Electrical

Frequency:	40 GHz to 50 GHz
Voltage	9.5 Kv
Beam current	25 mA
Ouput power (assuming 5% beam efficiency)	12 Watts

The circuit design was chosen to follow similar helix design for millimeter applications. The propagation parameter γa was selected to

$$\gamma a = 1.6 \text{ (at 42 GHz)}$$

The circuit parameters are as follows:

Helix Circuit

Helix wire (tungsten tape) 0.004 in. x 0.010 in. (for BN rods: 0.0025 in. x 0.010 in.)

Helix iD 0.026 in.
OD 0.034 in. (for BN rods: 0.031 in.)
pitch 0.018 in.

Support rods: width 0.012 in.

Circuit shell iD: 0.087 in. (with copper sleeve 0.005 in. thick)

Circuit length: 1.000 in. (20 wavelengths at 44 GHz)

Helix Assembly

The helix circuit is assembled inside the integrated pole piece tube envelope with the heat shrink assembly techniques. The helix support structure and the tube envelope have to be precision-sized to provide an accurate interference fit, that determines the compression forces and contact pressures. It is possible to analyze[22] the interference fit stresses and deformations on the basis of a simplified model. The contact pressures between helix and rods can then be predicted as a function of the interference fit as shown in Figure 15.

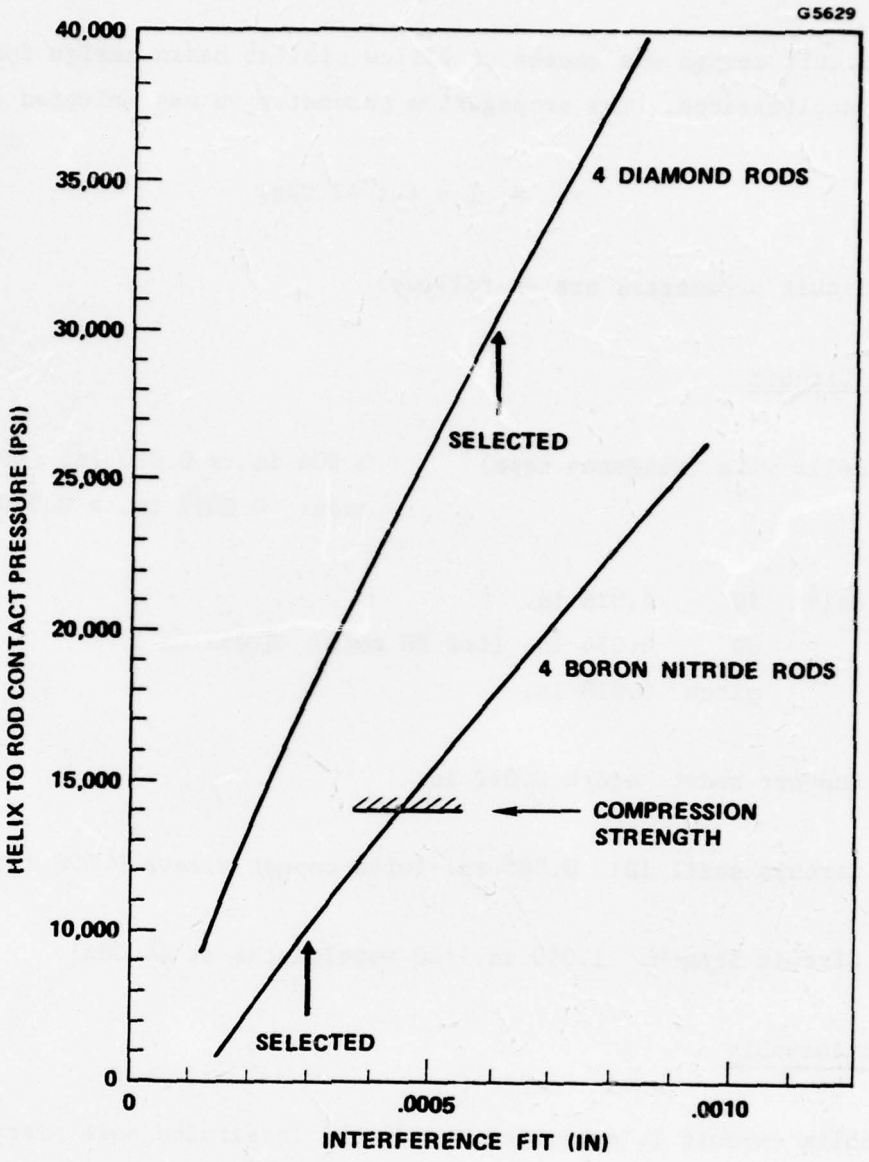

Figure 15 Predicted contact pressure on millimeter wave helix as function of interference fit.

The compression strength P_c of Boron Nitride is

$$P_c \text{ (Boron Nitride)} = 14{,}000 \text{ psi}$$

the interference fit ΔI for the Boron Nitride supported helix tester has therefore been selected to

$$\Delta I = 0.0003 \text{ in.}$$

corresponding to a contact pressure of 10,000 psi. The interference fit for the diamond supported helix and the Beryllia supported helix has been selected to

$$\Delta I = 0.0006 \text{ in.}$$

corresponding to an estimated contact pressure of 30,000 psi. Compression strengths P_c of these materials is much higher:

$$P_c \text{ (Beryllia)} = 200{,}000 \text{ psi}$$

$$P_c \text{ (diamond)} = 1{,}000{,}000 \text{ psi}$$

Focusing Design

The PPM focusing design for the equivalent millimeter helix TWT provides:

Focusing peak field $B_p = 2760$ gauss

(Thermal) plasma wavelength $\lambda_{+H} = 0.944$ in.

Focusing period	$2\ L_m = 0.240$ in.
Focusing stiffness	$\frac{\lambda_{+H}}{2\ L_m} = 3.92$

The pole piece configuration has been determined (for Samarium Cobalt magnets) as follows:

Pole piece thickness	0.030 in.
Magnet thickness	0.090 in.
Pole piece ID	0.097 in.
Magnet iD	0.150 in.
Pole piece (magnet) OD	0.400 in.

This configuration has been incorporated (without magnets) into the millimeter helix tester design.

The helix assembly with pole pieces and optical window is shown schematically in Figure 16.

Conduction Cooling

The tube envelope is conduction-cooled by the pole pieces and by inter-pole piece heat risers. These are 2 radial copper bars that are attached on opposite sides to the copper spacers between the iron pole pieces. The millimeter helix testers are mounted in a test fixture that simulates a conduction-cooled tube package. The test fixture clamps both the pole pieces and the heat risers so that good heat transfer from the tube body is achieved. The test fixture is attached to a cooling plate (heat sink). A schematic of the helix tester mounted in the test fixture is shown in Figure 17. The temperatures on the heat-riser (T_1) and on the package (T_2) are monitored with thermocouples.

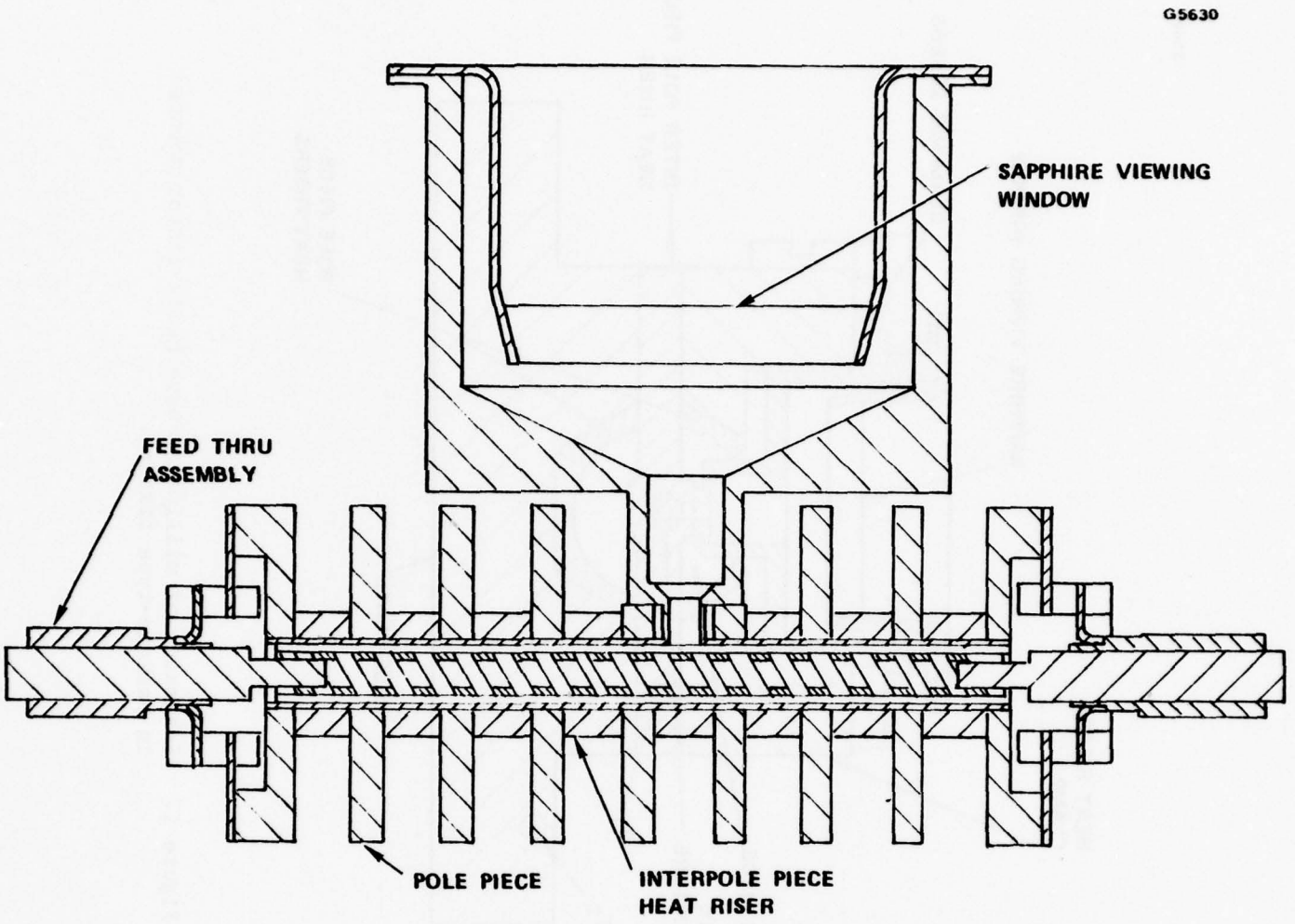

Figure 16 Schematic of millimeter helix testers with DC-couplers and viewing window.

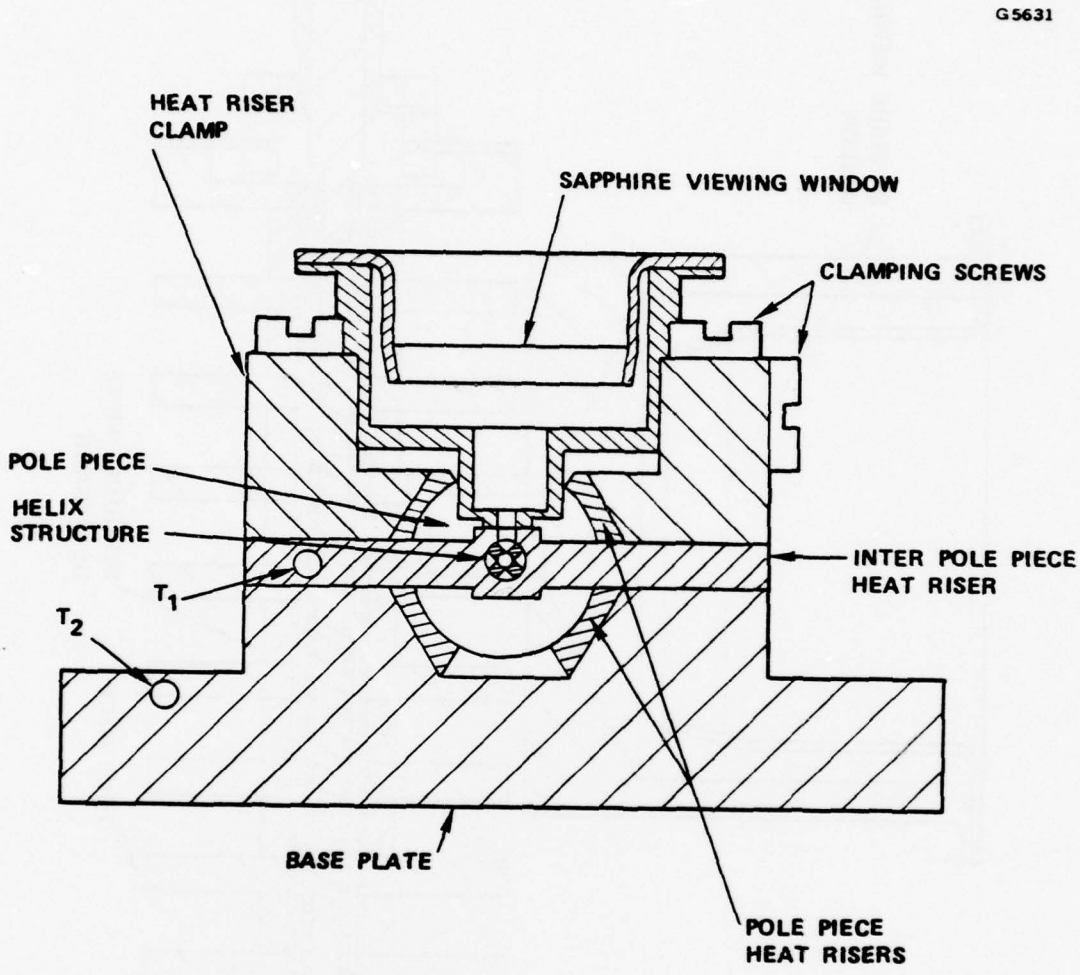

Figure 17 Schematic of millimeter wave helix tester mounted in package-type fixture.

Helix Couplers

Several of the millimeter helix testers were equipped with RF-couplers for the purpose of making loss measurements and for thermal evaluation of the circuit with RF. In this case the circuit is to be driven with a high millimeter power source and the circuit losses would provide the thermal load.

The RF coupler consists of a waveguide window, a tapered waveguide transformer, which provides a transition to a waveguide of reduced height, and a coupler post connected to the helix. The RF-coupler configuration is shown schematically in Figure 18. The coupler design has been optimized with a cold test structure scaled to X-band (4:1). The cold test structure provided a movable backwall (short) and an adjustable height of the antenna post, so that the match can be optimized. The resultant optimized match is shown in Figure 19. This coupler design was implemented in the millimeter helix testers with the provision, that the backwall position remains variable and so that it can be optimized for each of the millimeter helices with different support rods. The resultant match on a millimeter helix tester with Boron Nitride rods is shown in Figure 20. RF-transmission loss at 45 GHz on this tester was found to be more than 20 dB, which indicates excessive RF-leakage, presumably at the optical window. Further RF-evaluation of the millimeter helix testers appeared therefore as not very meaningful, since the circuit losses could not be determined accurately.

Construction of Millimeter Helix Testers

Construction and assembly of the millimeter helix testers used the same methods and procedures as for high power helix traveling wave tubes, including a vacuum bakeout. The diamond support rods were assembled with relatively small diamond bars that were metallized and bonded to

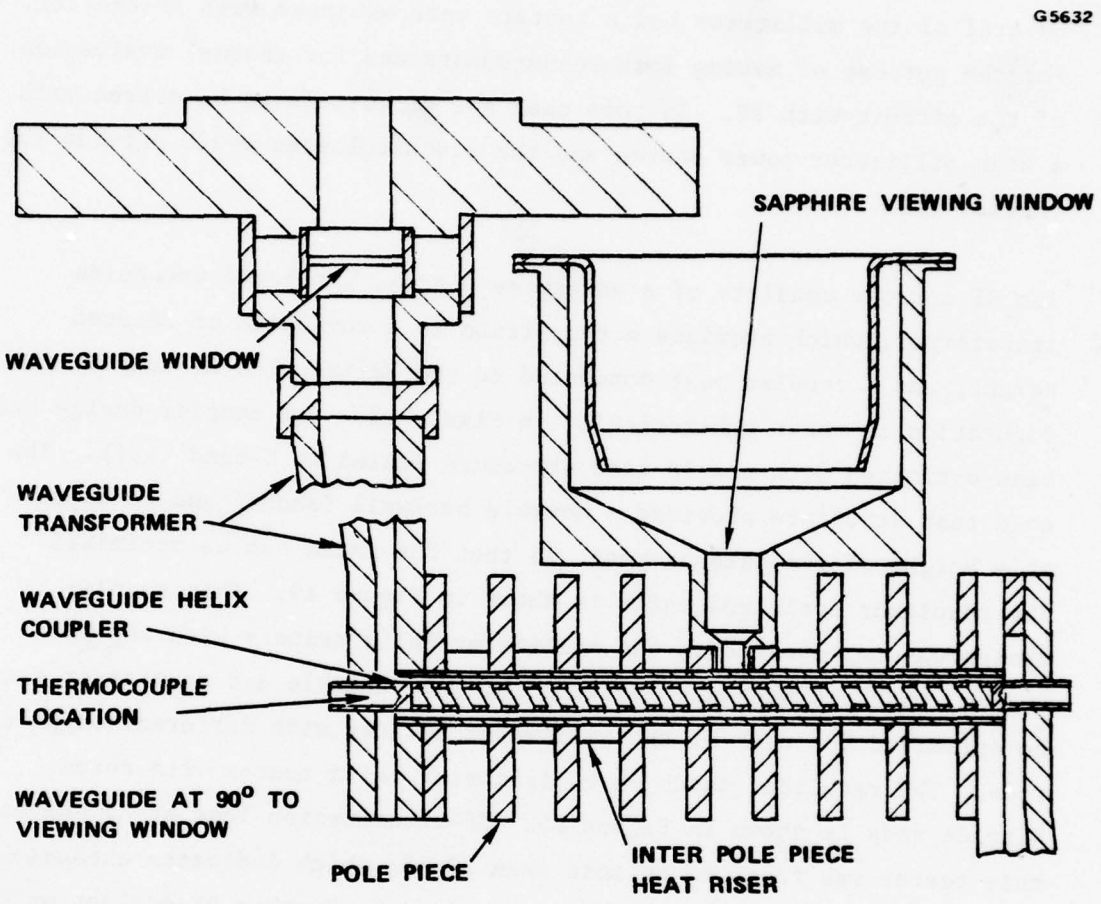

Figure 18 Schematic of thermal millimeter helix tester with RF-waveguide coupler and window.

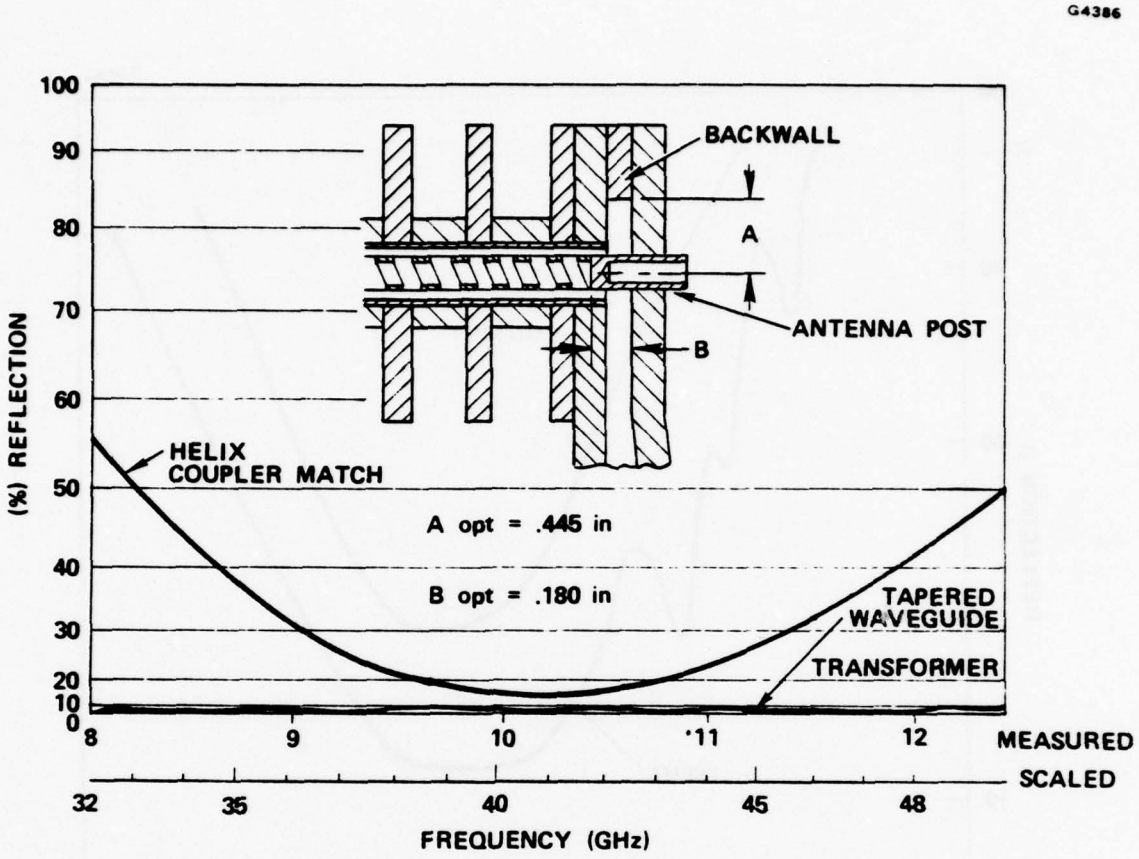

Figure 19 RF coupling of helix to waveguide with optimized back wall and antenna position (measured).

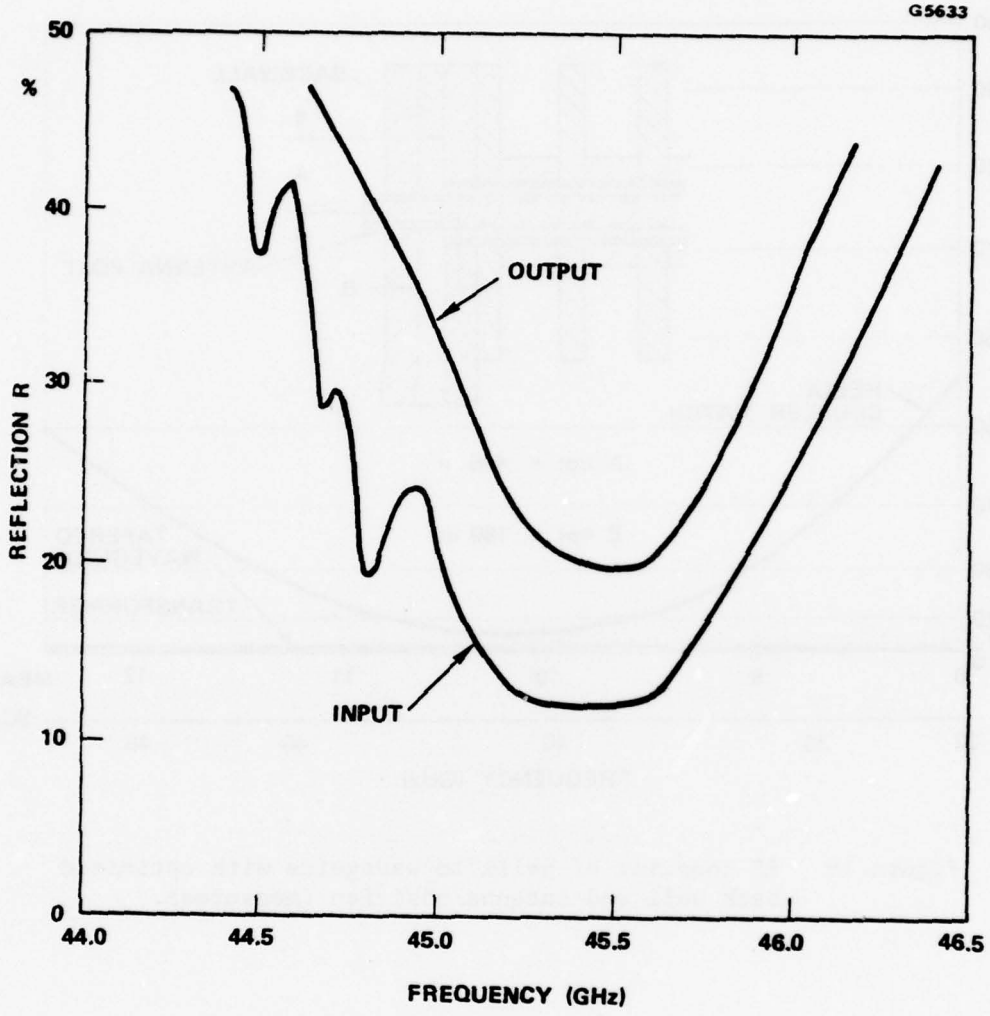

Figure 20 RF-coupling of helix to waveguide for millimeter helix tester with Boron Nitride rods (measured).

a copper strip. Figure 21 shows a picture of a diamond bar with a metallized edge. Figure 22 shows the assembled diamond rod. Metallizing and bonding techniques are the same as used for diamond heat-sink applications.[23] Such bonds are known to provide excellent heat transfer[24], and the bonded rod structures facilitate the heat shrink assembly. The Beryllia rods were therefore also bonded to a copper strip. Figure 23 shows a picture of all three types of rods used for the millimeter helix testers. The cross-section of the rods is rectangular. The outside surface of the rods was rounded with a sizing tool to match the inside curvature of the tube envelope. The inside surface of the Boron Nitride rods was also contoured to match their curvature to that of the helix, while the inside surfaces of the diamond and Beryllia rods were flat. For these rods the helix was ground along the axis to provide flat supporting surfaces for the rods.

A number of special fixtures and tools are required for the "sizing" operation on a helix circuit and for the heat shrink assembly of high power helix structures. These were adapted for the assembly of the millimeter helix testers. It was found, however, that these were not adequate for the much higher precision required of millimeter structures. Tolerances in the interference fit were excessive, and it would then not have been possible to assure the necessary contact pressures. Some of the fixtures had to be modified to remedy this problem, and adequate interference fit tolerances were then obtained.

Figure 24 shows a picture of a partially assembled millimeter helix tester with viewing window, dc-couplers and heat risers. Figure 25 shows the tester completely assembled.

Figure 26 shows the millimeter helix tester with waveguide window and waveguide transformer. A picture of the millimeter helix tester mounted in the conduction cooled test fixture is shown in Figure 27.

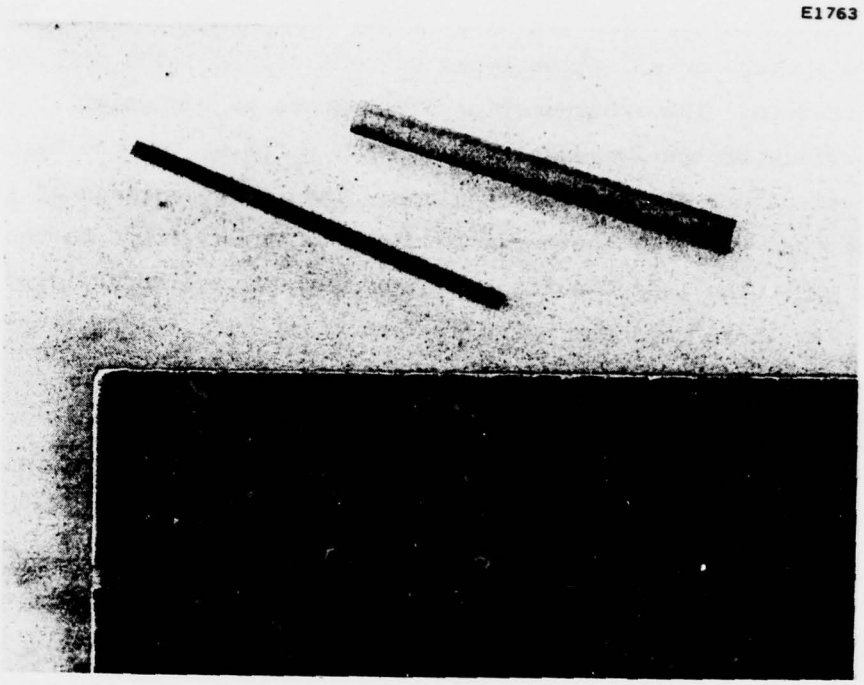

Figure 21 Picture of diamond bar with metallized edge.

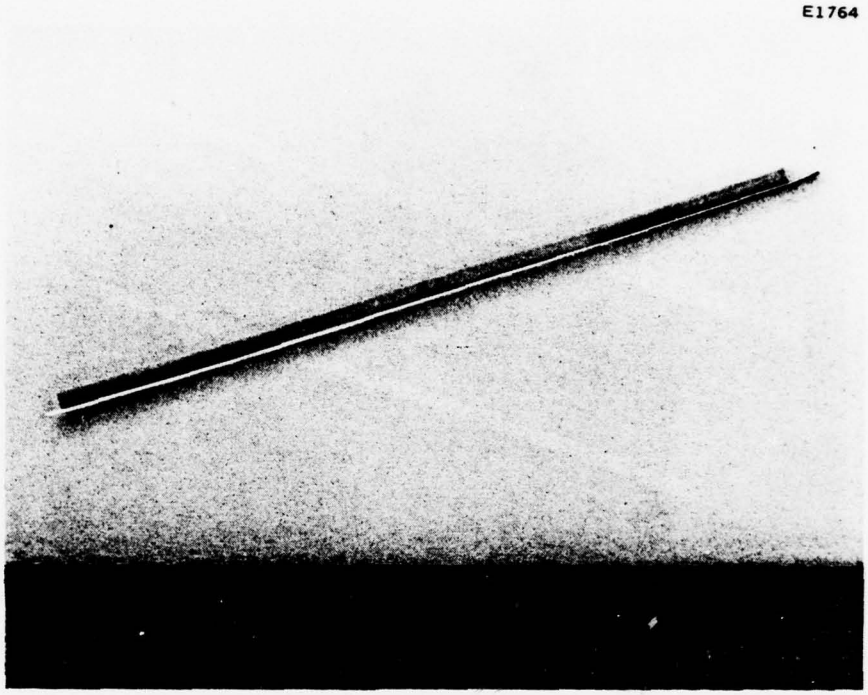

Figure 22 Picture of assembled diamond rod with copper strip.

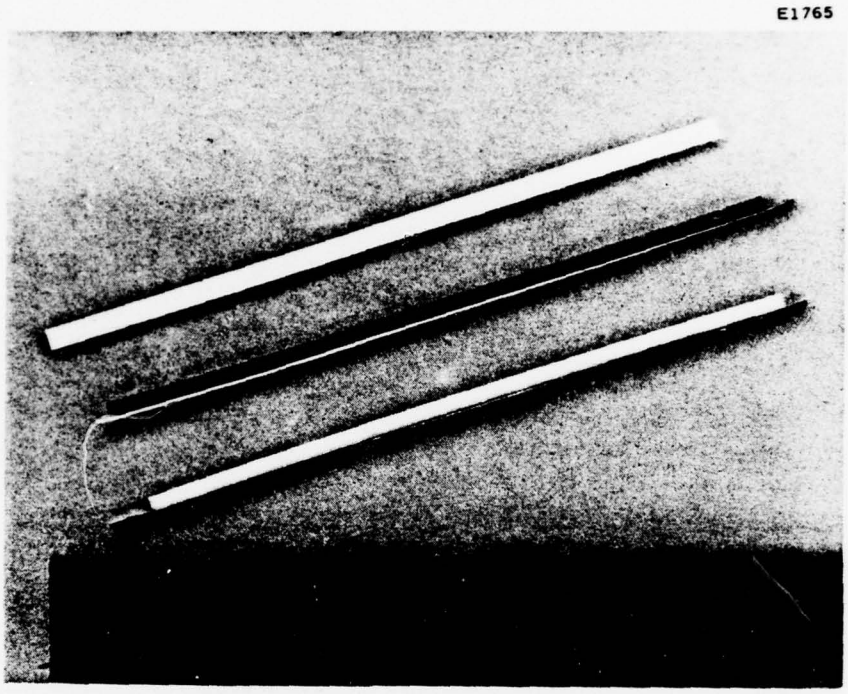

Figure 23 Picture of three types of ceramic rods used for the millimeter helix testers: boron nitride rod, assembled diamond rod, and beryllia rod bonded to a copper strip.

E1766

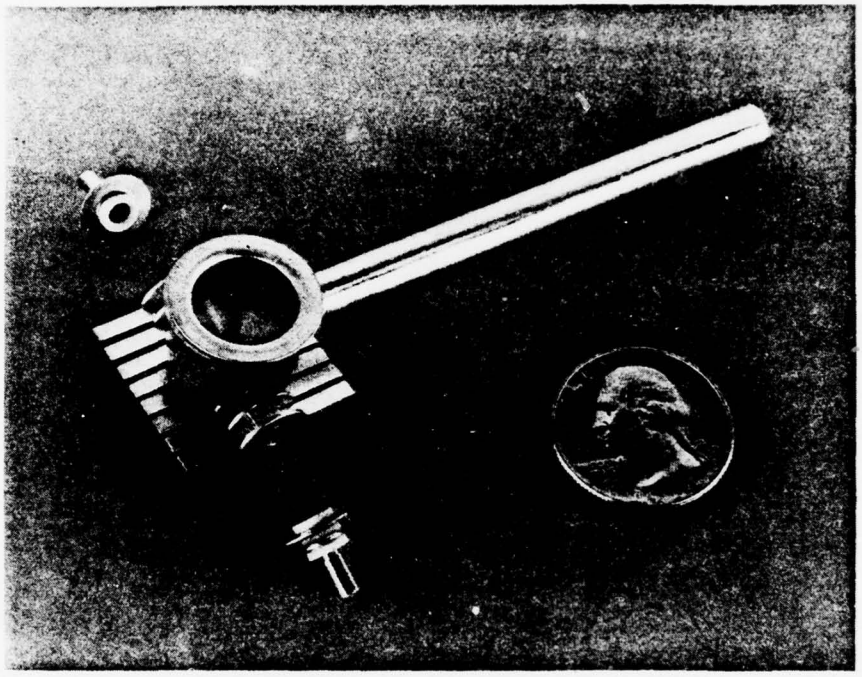

Figure 24 Picture of partially assembled millimeter helix tester with viewing window, dc-couplers and heat risers.

E1854

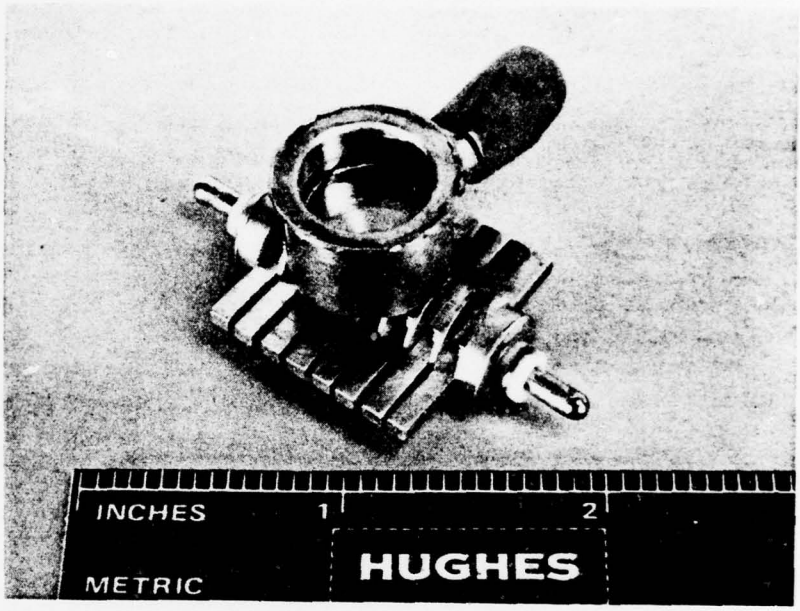

Figure 25 Picture of assembled thermal millimeter helix tester for dc.

E1767

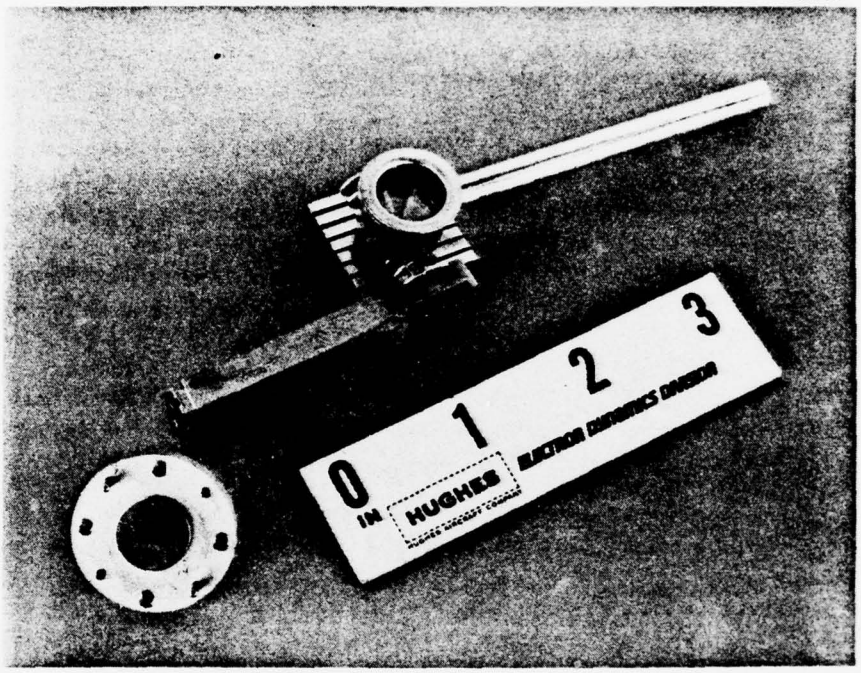

Figure 26 Picture of millimeter helix tester with waveguide window and waveguide transformer.

E1855

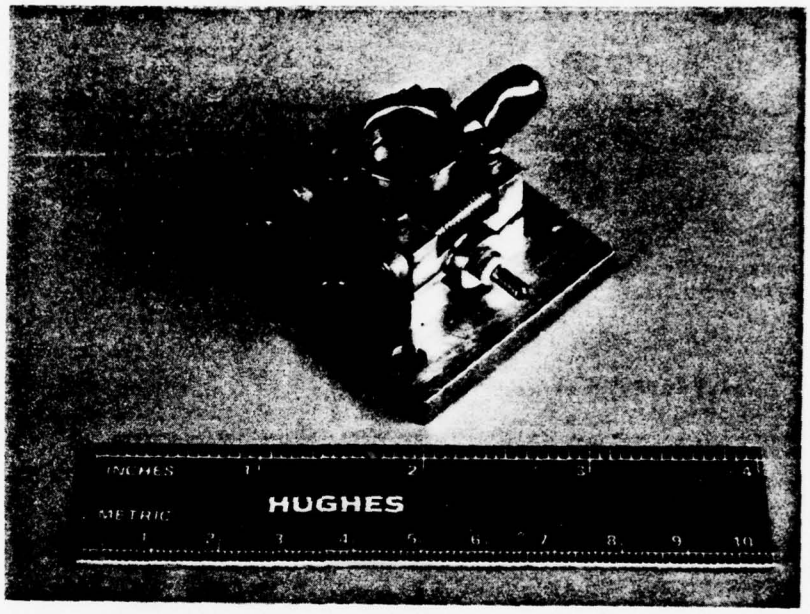

Figure 27 Picture of millimeter helix tester mounted in conduction cooled package test fixture.

The construction of three millimeter helix testers was completed. Two of these used Boron Nitride rods, one for dc-testing and one with RF couplers. The third tester used diamond rods and was initially constructed with RF-couplers, but was later modified for DC-thermal evaluation. The construction of a millimeter helix tester with Beryllia rods was initiated also, but was not completed because the rods were damaged in the process of the heat-shrink assembly.

4.2 THERMAL EVALUATION OF MILLIMETER HELIX TESTERS

Two of the millimeter helix testers were evaluated thermally, one with Boron Nitride rods and one with diamond rods. An RF-thermal evaluation was not attempted because it was not possible to determine the actual value of the RF losses. For the dc-evaluation a voltage was applied to the helix, so that its resistance served as thermal load. The average helix temperature can then be determined from the change in resistivity of the helix wire that is a known function of temperature.

Figure 28 shows thermal data of the Boron Nitride helix tester. The helix burned out at a thermal helix load of 33 Watts. At this condition the average helix temperature was 700°C. The copper coating of the helix had then disappeared. The burn-out condition must have occurred due to a hot spot on the helix wire, since the melting temperature of tungsten is nearly 3400°C. Although the burn-out load of the helix tester was 33 watts, the maximum permissible helix load is lower. This is because a helix temperature of 700°C is considered excessive, especially for helices with copper coating. If a maximum helix temperature of 400°C to 500°C is acceptable, the maximum permissible helix load would be 25 watts/in. to 31 watts/in. It is estimated that a helix tube for 30 watts to 40 watts power output in the 40 GHz to 50 GHz range would produce such a thermal load.

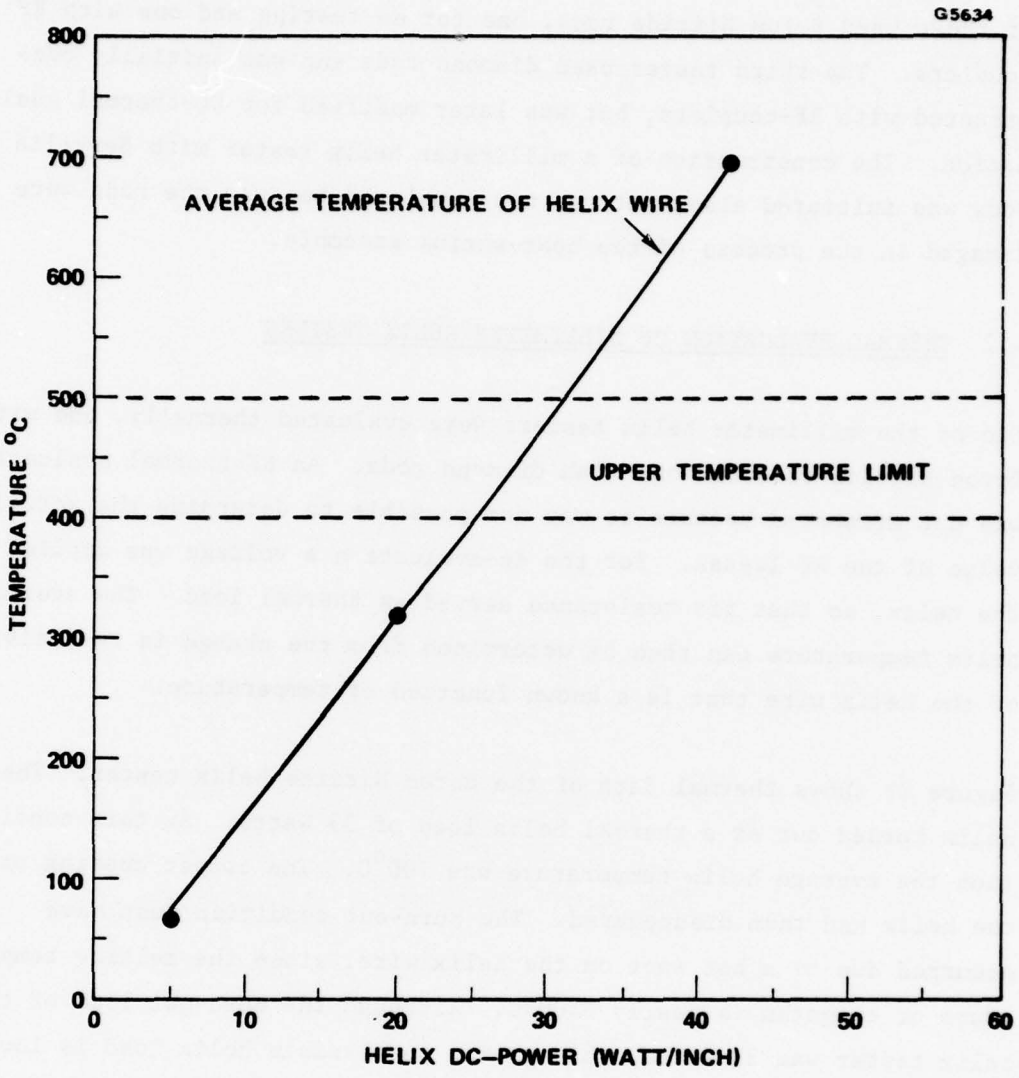

Figure 28 Thermal loading of millimeter helix tester with Boron Nitride support rods (measured).

The thermal data of the diamond helix tester are given in Figure 29. The average helix temperatures, as well as the temperatures on the heat-riser and on the package (see Figure 17) are shown as a function of the helix load. The test was carried to a power load of 132 watts, or 165 watts/in. At this load the average helix temperature was 380°C. A break in the wiring lead to the erroneous conclusion of a helix burn-out. Later inspection of the tester showed no visible damage to the helix wire or its coating. The diamond helix structure has therefore been demonstrated to handle helix power loads in the range of 180 watts/in. to 250 watts/in., corresponding to permissible helix temperatures from 400°C to 500°C. Helix tubes with output power levels in the order of 100 watts to 200 watt CW in the 40 GHz to 50 GHz range appear therefore feasible, when diamond support rods are used.

These data demonstrate the outstanding heat transfer capability of diamond used as dielectric support for helix structures; especially for millimeter wave applications. Although this has been recognized before[25], there were problems to incorporate diamonds into a helix structure. This is because diamonds are only available in very small sizes, and it is difficult and expensive to shape diamonds (by polishing) to a desired configuration. In the previous application each turn of an X-band helix was supported by individual diamond stubs utilizing both compression and brazing techniques.

It should be mentioned, however, that the power capability for such millimeter helix structures could be much larger when deficiencies in the heat transfer assembly are eliminated (Section 5).

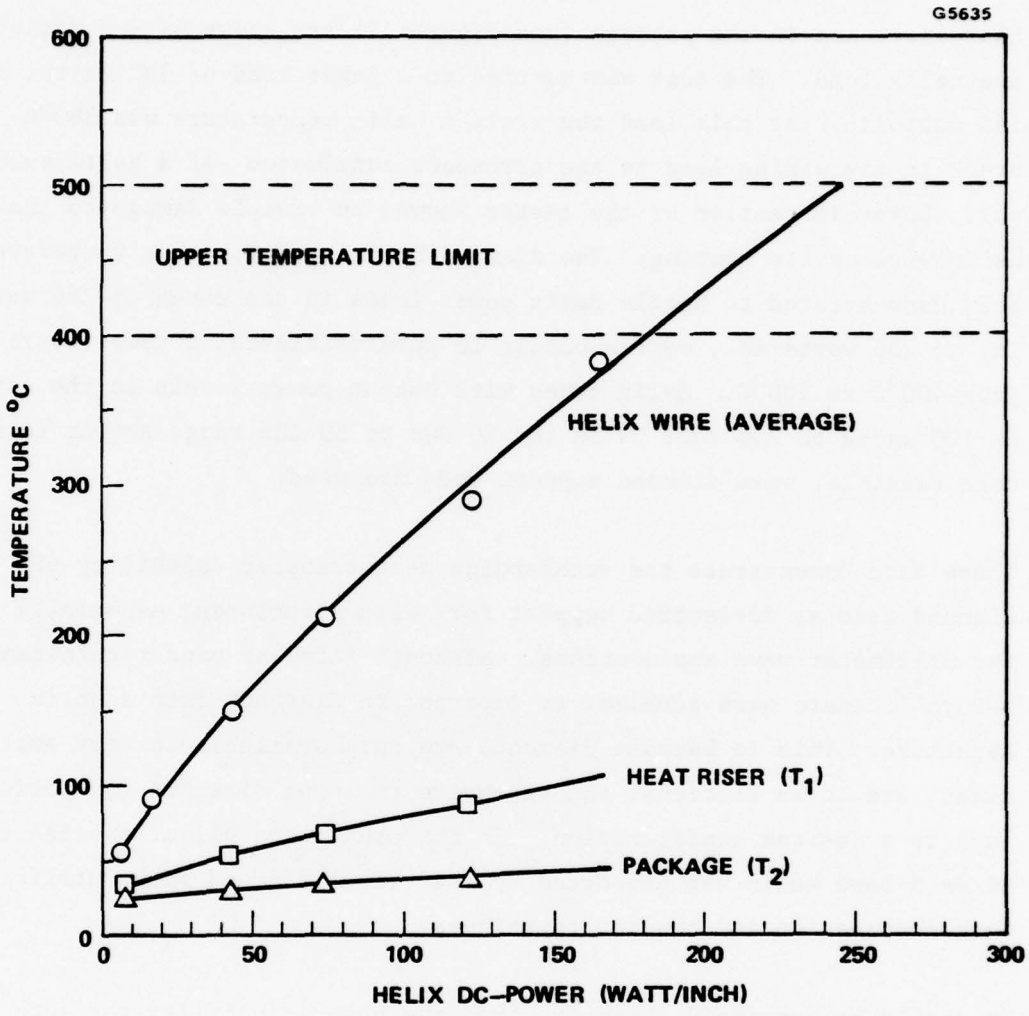

Figure 29 Thermal loading of millimeter helix tester with diamond support rods (measured).

5.0 PREDICTED OPTIMUM PERFORMANCE OF MILLIMETER HELIX STRUCTURES

The heat transfer and thermal conductivity data obtained with the thermal tester make it possible to estimate the thermal power capability of a high power helix traveling wave tube. This has not been possible so far since quantitative data on heat transfer of interfaces have not been available previously. Power estimates had to depend on empirical results of hot tubes that provided no information on deficiencies or possible improvements.

Thermal power capability estimates can be made with these data when the geometry of the structure, the surface conditions of the interface and their contact pressures are known.[26] It also has to be assumed, that such interfaces are flat and parallel.

In a high power helix tube several sources of waste power are dissipated in the structure. This power has to be removed in order to keep operating temperatures within acceptable limits. Figure 30 depicts schematically the waste sources of concern. These can be listed as:

1. Q_B beam interception
2. Q_W helix wire RF-losses
3. Q_D dielectric RF-losses
4. Q_{Sh} helix shield losses

Beam interception can generally be estimated from empirical data of similar tubes, and from the quality of the focusing design. The sum of the RF-losses, Q_L

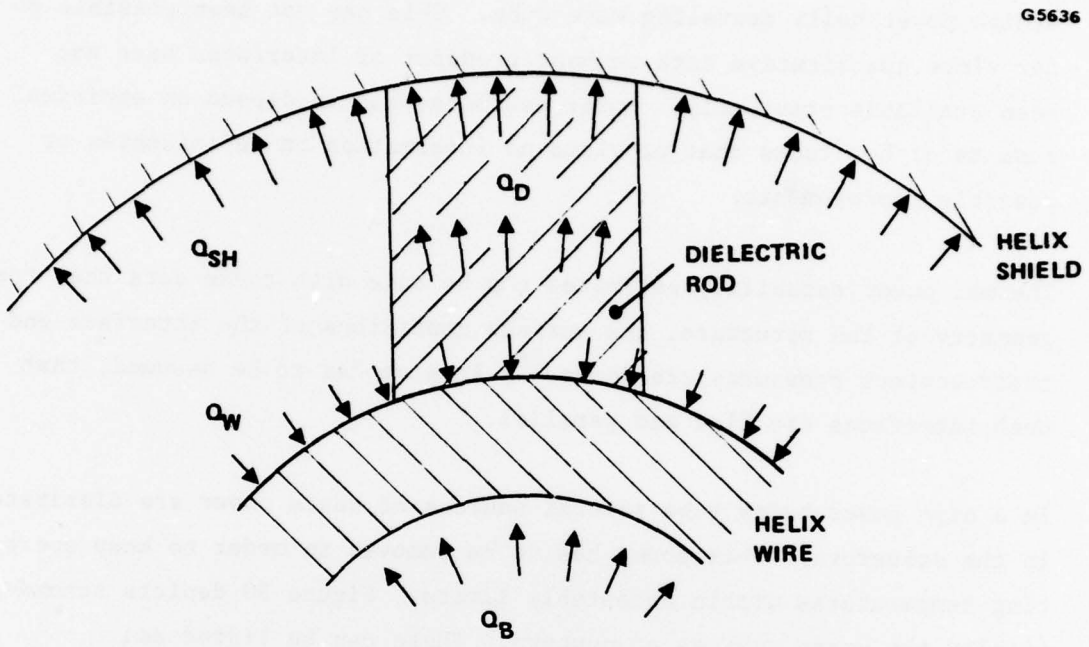

Figure 30 Schematic of waste heat sources in a helix structure.

$$Q_L = Q_W + Q_D + Q_{Sh}$$

can be obtained from loss measurements on a circuit structure, but the relative contributions of each of the loss sources are generally not known. It is however well known that these losses become large with higher frequencies, especially up in the millimeter region. The wire losses and shield losses are skin effect losses and increase with the square root of frequency, while the dielectric bulk losses increase proportional with frequency and become very substantial in the millimeter region. The shield losses Q_{Sh} are usually of little concern in thermal respects, even if they are relatively large, because of good heat conduction through the tube envelope. The dielectric losses are also generally not a limiting factor in the power capability of a traveling wave tube, other than they may rapidly increase RF-losses at higher power levels due to poorer heat flow in the ceramics at higher temperatures. The power capability is therefore primarily limited by the helix wire and its waste loads, the helix interception and the helix wire RF-losses. Even though commonly used helix wire materials have very high melting temperatures (tungsten 3400°C, molybdenum 2600°C), it is not permissible to operate helix wires at higher than 400°C to 500°C. This is because very often such helix wires are copper coated to reduce wire RF losses, and this copper coating starts to evaporate at temperatures higher than 500°C. Even without copper coating the helix temperatures are similarly limited because of excessive vapor pressures at higher temperatures and the destructive effects of the resultant ionization on focusing and tube life. The maximum permissible temperature gradient ΔT from the helix to the tube envelope is therefore limited to about

$$\Delta T_{max} \approx 300^{\circ}C$$

depending on the type of cooling.

The heat flow Q/per unit length has to pass from the helix wire to the tube envelope through a thermal resistance per unit length R_{th} producing a temperature gradient ΔT of

$$\Delta T = R_{th} \cdot Q$$

The thermal resistance[26] of the helix structure R_{th} consists of a series of thermal resistances as shown in the heat flow model of Figure 31, where

R_H = thermal resistance of helix wire per unit length

R_{Hc} = thermal interface resistance helix wire - ceramic support per unit length

R_C = thermal resistance of ceramic support per unit length

R_{CE} = thermal resistance of interface ceramics-envelope per unit length

The maximum permissible power load on the helix is then

$$Q_{max} = \frac{\Delta T_{max}}{R_{th}}$$

Values for the thermal resistances of the structure can be calculated for a given configuration, known conductivity k and heat transfer data h as obtained from measurements described in Section 3. Assuming a helix structure with the configuration

Helix tape wire thickness t
width w

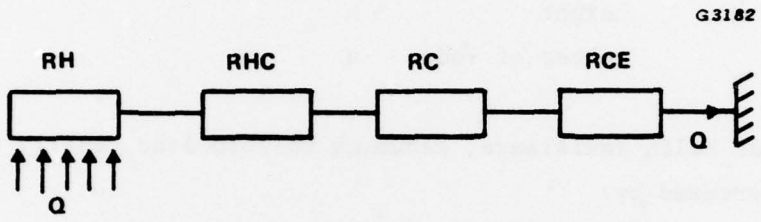

Figure 31 Heat flow model for helix structure.

Helix	ID	dai
	OD	dao
	pitch	P
	length	L
Shield	ID	d_s
Rods	width	b
	height	h
	number of rods	n

The thermal helix resistance, assuming uniform load density on the wire, can be expressed by:

$$R_H = \frac{1}{k_H} \frac{(dai + dao)\ \pi\ P}{64 \times n \times W \times t \times L}$$

the interface resistance helix-support rods is

$$R_{HC} = \frac{1}{h_{Hc}} \frac{P}{n\ (W \times b) \times L}$$

the thermal resistance of the support rods is given by:

$$R_C = \frac{1}{k_c} \frac{2hP}{(W + P) \times b \times n \times L}$$

provided the heat flow spreads linearly in the axial direction from the helix contact to the shield.

The thermal interface at the shield is

$$R_{CE} = \frac{1}{h_{CE}} \cdot \frac{1}{n \times L \times b}$$

The maximum power capability per unit length can then be estimated for the millimeter helix testers with the selected dimensions and materials (Section 4.1) under the assumption of optimum interface conditions and large contact pressures (10,000 psi for interfaces with copper or Boron Nitride and 20,000 psi for interfaces with other materials). The results are summarized in Table I, including those for a composite ceramic helix with plasma-sprayed Beryllia and a copper helix. The maximum helix temperature T_H has been assumed to $T_{Hmax} = 400^{\circ}C$, while the maximum temperature gradient from helix to shield ΔT is assumed to

$$\Delta T_{max} = 300^{\circ}C.$$

The power capability of a diamond supported helix is thus found to be about 2.5 times as high as that of a Beryllia supported helix, and three times higher than that of a similar Boron Nitride supported helix. A composite ceramic helix structure, on the other hand, promises to have a thermal capability, comparable or better to that of a diamond supported helix. For the power levels considered, the temperature gradients along the diamond are moderate, while the temperature gradients along the helix wire are large. A larger cross section of the helix wire would therefore be desirable.

The predicted value of 1179 watt/in. for a millimeter helix with diamond support is found to be substantially larger than the experimental data, indicating that large further improvements should be possible with improved assembly techniques.

One experimental millimeter helix tester failed due to hot spots on the helix wire, probably caused by cracks and fissures in the helix wire. Although this problem should be remedied with better methods of wire fabrication and quality control, it is not the limiting factor in the power capability of these testers. From the average temperature data on the helix wire it becomes apparent that thermal interface resistances are not nearly as low as expected. It is likely that flatness and parallelism is not adequately maintained, and the contact pressures may not be high enough due to excessive tolerances in sizing and of the interference fit.

6.0 SUMMARY AND CONCLUSIONS

The thermal properties of materials suitable for millimeter wave helix structures have been evaluated with a test apparatus using an infrared microscope. This equipment measures heat transfer properties between different materials as a function of pressure, as well as thermal conductivities of materials as a function of temperature.

It was found that the heat transfer between different materials is very critically dependent on flatness and parallelity of the contact surfaces. The heat transfer improves substantially with higher contact pressures, with pressures of at least 20,000 psi. Heat transfer is also found to be better when the contacting surfaces have a high quality microfinish (polish), at least for hard materials. However, when one of the materials is copper, a lower grade of microfinish of the surface is preferable.

Such data have not been available previously and can be used for the thermal design and analysis of high power helix structures.

Measured conductivity data of ceramic materials, such as diamond IIA, Beryllia and anisotropic Boron Nitride agree well with predictions.

Several helix structures for the 40 GHz to 50 GHz range were constructed with these materials for thermal evaluation. The helix structure with diamond support achieved a power capability of 165 Watts/in. on the helix, while the average helix temperature was 380^{o}C. These data demonstrate that helix tubes in the 40 GHz to 50 GHz range can be constructed for 100 Watt to 200 Watt CW power output, using a practical helix assembly with diamond support.

Analysis of the heat transfer data indicate that further significant improvements should be possible with refined assembly and construction techniques.

TABLE I

ESTIMATED MAXIMUM THERMAL CAPABILITIES OF MILLIMETER HELIX STRUCTURES
(Assuming $TH_{max} = 400^{o}C$, $\Delta T_{max} = 300^{o}C$)

Structure

		Diamond Rods	Beryllia Rods	Boron Nitride Rods	Composite Ceramic Structure
Maximum helix temperature	TH_{max}	$400^{o}C$	$400^{o}C$	$400^{o}C$	$400^{o}C$
Temperature gradient in helix	ΔT_{H}	$116.9^{o}C$	$46.7^{o}C$	$61.9^{o}C$	$13.1^{o}C$
Contact pressure helix-rods	P_{HC}	20,000 psi min	20,000 psi min	14,000 psi max	-
Temperature-gradient helix-rods	ΔT_{HC}	$60.6^{o}C$	$44.1^{o}C$	$95.8^{o}C$	0
Surface helix-rods		polished/polished	polished/polished	ground/ground	(ground)
Temperature gradient rods	ΔT_{C}	$50.7^{o}C$	$202.3^{o}C$	$119.0^{o}C$	$265.1^{o}C$
Temperature gradient rods (ceramic) - shield	ΔT_{CS}	$71.8^{o}C$	$6.9^{o}C$	$23.3^{o}C$	$21.8^{o}C$
Contact pressure rods (ceramic) - shield	P_{CS}	10,000 psi min	10,000 psi min	10,000 psi min	10,000 psi min
Maximum power capability	Q_{max}	1179 W/in.	471 W/in.	411 W/in.	1556 W/in.

LIST OF REFERENCES

1. W. Friz, "Radio frequency power limitations for octave bandwidth traveling wave tubes." Techn. Rept. AFAL-TR-73-283 WPAFB, Nov. 1973

2. J. P. Laico, H. L. McDowell, C. R. Moster, "Medium-power traveling-wave tube for 6000-MC radio relay." B.S.T.J., Vol 35, Nov. 1956 (p. 1285-1346)

3. A. H. Iverson, "High average power dissipation in helix tubes." PGED, Vol 7, No. 2, April 1960 (p. 74-77)

4. F. Wray, J. R. Dawsey, "An experimental 1 KW CW helix traveling-wave tube for 5 - 10 gc/s." SERL, Techn Journal, Vol 15, No. 3, Oct. 1965

5. G. Fleury, P. Gosset, G. Kantorowitz, "CW X-band 1 KW helix TWT." MOGA 1970, Amsterdam, Sept. 1970

6. R. F. Russel, O. F. Doehler, "Composite metal ceramic helix." Tech. Report AFAL TR-77-206, Nov. 1977, WPAFB/Northrop Corp., Des Moines, Ill.

7. D. J. McKinzie Jr., "Simplified method for calculating thermal conductance of rough, nominally flat surfaces in high vacuum." NASA TND-5627, Jan 1970, Lewis Res. Center

8. M. M. Yovanovich, H. Fenech, "Thermal contact conductance of nominally flat, rough surfaces in a vacuum environment." Progress in Astronautics and Aeronautics, Vol 18, Academic Press 1966 (p. 773-794)

9. M. L. Minges, "Heat transfer across non-metallic interfaces at high temperatures." Report Air Force Materials Laboratory 1968

10. H. Fenech, W. M. Rohsenow, "Prediction of thermal conductance of metallic surfaces in contact. Transactions ASME Feb. 1963 (p.15-24)

11. N. D. Wells, E. A. Ryder, "Thermal resistance measurements of joints formed between stationary metal surfaces." Transactions ASME, April 1949 (p. 259-267)

12. E. M. Fry, "Measurements of contact coefficients of thermal conductance." AIAA Conference, Monterey, Ca., Sept 1965 (p. 719-734)

13. E. Fried, M. J. Kelley, "Thermal conductance of metallic contacts in a vacuum." AIAA Conference, Monterey, Ca., Sept. 1965 (p. 697-718)

14. B. Mikic, G. Cornascialli, "The effect of thermal conductivity of plating material on thermal contact resistance." ASME Conference, Los Angeles, Nov. 1969

15. E. Fried, F. A. Costello, "Interface thermal contact resistance problem in space vehicles." ARS Journal, Feb. 1962 (p. 237-243)

16. R. W. Powell, C. Y. Ho, P. E. Liley, "Thermal conductivity of selected materials." Purdue University, Nov. 1966

17. W. Espe, "Materials of high vacuum technology." Pergamon Press, 1968

18. Leypold, K. Diels, R. Jaeckel, "Vacuum Handbook", Pergamon Press, 1966

19. L. H. Van Vlack, "Physical ceramics for engineers." Addison-Wesley 1964

20. Batelle Inst., "Engineering properities of selected ceramic materials." Batelle Inst., 1966

21. Y. S. Touloukian, "Thermophysical properties of high temperature solid materials." Purdue University, McMillan Co., 1967

22 C. T. Wang, "Applied elasticity." McGraw Hill Co., N.Y. 1953 (p. 54-58)

23. M. Seal, "A review of methods of bonding or making electrical contacts to diamond." Engelhard Industries Tech. Bulletin, June 1969

24. P. R. W. Hudson, "The thermal resistivity of diamond heat-sink bond materials." J. Phys. D., Vol 1976, (p. 225-232)

25. R. Harper, U. Pittack, "Diamond as support material for TWT-helices." IEDM Conference, Washington, D.C., Dec. 1976

26. J. A. Lucken, "Some aspects of circuit power dissipation in high power CW-helix traveling-wave tubes." Part I, IEEE Trans. ED, Vol G, No. 9, Sept. 1969 (p. 813-820)

MISSION
of
Rome Air Development Center

RADC plans and conducts research, exploratory and advanced development programs in command, control, and communications (C³) activities, and in the C³ areas of intelligence, reliability and compatibility of electronic systems. The principal technical mission areas are communications, electromagnetic guidance and control, surveillance of ground and aerospace objects, intelligence data collection and handling, information system technology, ionospheric propagation, solid state sciences, microwave physics and electronic reliability, maintainability and compatibility.